

MINISTRY OF EDUCATION AND SCIENCE OF UKRAINE

National Aerospace University
«Kharkov Aviation Institute»

Faculty of Aircraft Engineering

Airplane and Helicopter Design Department

Explanatory Note to Diploma Project of

Master

(degree)

Subject: **Design of a system for increasing the lifting force of the wing of a medium-range passenger aircraft**

XAI.103. 160fd.23S.134.06.19 EN

Applicant of 2 Year 161FD Group

Field of knowledge 13

Mechanical Engineering

Specialty: 134 Aerospace

Engineering

Educational program: _____

Airplanes and helicopters

He Shuyuan

(name)

Supervisor: Sergey Filipkovskij

(name)

Reviewer S.M. Ivanov

(name)

**Ministry of Science and Education of Ukraine
National Aerospace University
«Kharkiv Aviation Institute»**

Faculty Aircraft Engineering
Department 103 Airplane and Helicopter Design
Degree First (Bachelor)
Field of knowledge 13 Mechanical Engineering
Specialty 134 Aerospace Engineering
(Code and name)
Educational Program Airplanes and helicopters
(Name)

**APPROVED by
Head of Chair**

PhD, Ass. Prof. Andrii HUMENNYI
“ ” 2023

**TASK
FOR DIPLOMA PROJECT**

Shuyuan He
(Name)

Subject of qualification paper Design of a system for increasing the lifting force of the wing of a medium-range passenger aircraft

Supervisor of qualification paper Sergey Filipkovskij, Prof., DSc
(name, degree, scientific degree)

Approved by University order No 413-уч from “ 20 ” 03 2023
Qualification paper presentation deadline 15/05/2023
Initial data for the qualification qualification L=6000 km; L_{TO}=2000 m;
H_{cruis}=12.5 km; V_{cruis}=955 km/h; V_{max}=1000 km/h; n_{crew}=5 pers; n_{pass}=189 pers.

Content of explanatory note (list of problems to solve)

Abstract

1 Design Section

1.1 Statistical designing of the aircraft shape

1.2 Technical Data

1.3 Three View Diagram

2 Research Section

2.1 General information about the wing lift system

2.2 Concept Design of Adaptive Wing with Flexible Trailing Edge

2.3 Design of wing geometric parameters

2.4 Wing and high-lift devices parameters influence on C_y

2.5 Wing and high-lift devices parameters influence on required starting thrust

3 Economics Section

Calculation of aircraft and engine operation cost and transportation cost of one cargo ton per kilometer.

Conclusion

References

List of drawings (with the exact indication of obligatory drawings)

- Master geometry of aircraft surface, general view drawing.
 - Load carrying structure layout of the aircraft.
 - 3D stereogram of the designed aircraft.
 - Wing transmission structure diagram.
-

Advisors of diploma project sections

Section	Name and duty of advisor	Signature, Date	
		Task is given	Task is submitted
1	Prof., DSc, Sergey Filipkovskij	10/02/2023	23/03/2023
2	Prof., DSc, Sergey Filipkovskij	10/02/2023	11/05/2023
3	Ass. Prof., PhD, Tatiana Pavlenko	10/02/2023	15/05/2023
4			
5			

Normative inspection _____ Sergey Filipkovskij « » _____ 2023
 (Signature) (Name)

Date when task is given _____ 2023 February 10 _____

CALENDAR PLAN

№	Diploma project milestones	Diploma project milestone deadlines	Notes
1	Design Section	23/03/2023	
2	Research Section	11/05/2023	
3	Economic Section	15/05/2023	
4			
5			

Applicant _____ Shuyuan He _____
 (Signature) (Initials and surname)

Supervisor of diploma project _____ Sergey Filipkovskij _____
 (Signature) (Initials and surname)

SUMMARY

This diploma project of the Master " Design of a system for increasing the lifting force of the wing of a medium-range passenger aircraft " contains 94 pages, 3 sections, 5 tables, 41 figures and 17 sources.

The object of study is to design a system for increasing the lifting force of the wing of a medium-range passenger aircraft.

The purpose of the work operational features of the passenger plane, to analyze the operation of the wing, to evaluate the feasibility of the designed aircraft, to calculate the cost of operating the aircraft.

Design and construction methods are mathematical, using empirical dependencies and the results of statistical data processing on existing prototype aircraft, as well as analytical, to use 3D software to model and catia software to simulate, and get the stress-strain diagram.

The results of the master's degree project:

The operational features of the passenger aircraft are analyzed;

The analysis of the operation of the wing structure of the aircraft;

The analysis of the technique to improve the lift of the aircraft;

The cost of operating the aircraft was calculated.

This thesis was done on a PC using the Microsoft office software. All calculations were performed in Microsoft 2016 software environments.

CONTENT

1. DESIGN SECTION	5
1.1 Statistical designing of the aircraft shape	5
1.1.1. Introduction	5
1.1.2. Development of technical task	6
1.1.3. Gathering and processing of the statistical data, their analysis	7
1.2. Technical Data	14
1.2.1. Aircraft tactical-technical requirements development	17
1.2.2. Selection and justification of the aircraft layout	17
1.2.3. Calculation of aircraft zero approximation take-off mass	19
1.2.4. Calculation of the structural mass of the main aircraft assemblies, power plant mass, fuel mass, mass of the equipment and controls	22
1.2.5. Engine selection and its characteristics	23
1.2.6. Determination of the basic geometrical parameters of the aircraft assemblies (fuselage, tail units, landing gear). Calculation of its center-of-gravity position. General view development.	25
1.2.7. Selection, justification, development and reconciliation of aircraft load-carrying structure	35
1.3. Three View Diagram	43
2. RESEARCH SECTION	45
2.1. General information about the wing lift system	45
2.1.1. Introduction of aircraft wing lift system	45
2.1.2. Research Inadequacies	47
2.2. Concept Design of Adaptive Wing with Flexible Trailing Edge	48
2.2.1. Introduction of Adaptive Wing with Flexible Trailing Edge	48
2.2.2. Drop-down hinge flap and spoiler offset configuration	48
2.2.3. Trailing edge flap variable camber technology	49
2.2.4. Intelligent flexible adaptive wing	50
2.2.5. Flexible ribbed adaptive wing concept	54
2.2.6. Kinematic study of rotatable wing rib mechanism	55

	4
2.3.Design of wing geometric parameters	59
2.4. Wing and high-lift devices parameters influence on C_y	62
2.5. Wing and high-lift devices parameters influence on required starting thrust.	66
2.6. Airplane parameters influence on power unit relative mass.	69
2.7. Airplane parameters influence on fuel relative mass	72
2.8. Airplane parameters influence on structure relative mass	74
2.9. Crew, equipment and payload mass calculation.	77
2.10. Airplane parameters influence on take-off mass	78
3. ECONOMIC SECTION	82
3.1. Calculation of aircraft and engine operation cost and transportation cost of one cargo ton per kilometer.	82
3.2. Conclusion	90
CONCLUSIONS	91
REFERENCES	92

1. DESIGN SECTION

1.1 Statistical designing of the aircraft shape

1.1.1. Introduction

The "MK10-200" aircraft is intended to serve as the foundation for a family of middle-seating passenger aircraft with two turbofan engines (CFM 56-7B27), high-quality design, and enhanced technological and operational mobility and unification.

The "MK10-200" aircraft is expected to have the following features:

- a) A broad range of functionality, which would include range, speed, seating capacity, comfort, regional autonomy, and airfield network;
- b) A wide range of variants according to application type mid-range, various kinds (foreign avionics and equipment);
- c) Modern operation and maintenance excellence;
- d) Conformance to contemporary flight safety requirements (AP-25, FAR-25, JAR 25), standards of quality, and cutting-edge ecological standards;
- e) Competitiveness with similar foreign prototypes.

The "MK10-200" aircraft is primarily intended for passenger, baggage, mail, and freight transportation on local routes with heavy

passenger traffic as well as on a few international routes that allow operating on both paved and unpaved RWY aerodromes.

The aircraft structure, its equipment, engines, other parts, and operations manuals must adhere to the following standards: aviation requirements AP-25 and additional requirements for the "EK20-200" aircraft's airworthiness, taking into account its design and operational features, which serve as the foundation for its certification.

1.1.2. Development of technical task

This section's goals are to build a broad framework and design for the passenger mid-range aircraft as well as to consider a potential version and design of the planned aircraft.

In addition, the development of KSS, the selection of an aerodynamic scheme, the approximation of the take-off mass and the calculation of the fundamental geometrical parameters of the aircraft are all being done concurrently. The primary tactical and technical requirements of the aircraft, as well as the aircraft's destination, are used as the initial data for the calculations, such as:

- Take-off distance (km) – 1.95;
- Flight range (km) – 5600;
- Cruise speed (km/hr) – 830;
- Cruise altitude (km) – 11.9;

- Number of passengers – 160;
- Type of engines (CFM 56-7B27).

The design task includes creating the new aircraft and each of its components. The aircraft's general layout was designed during the early design phase. In order to accomplish this, the basic tactical and technical requirements (TTR), allocated to the aircraft, flight specifications, diagrams, basic parameters, the general device of the aircraft and units, power plant (PP), binding of the basic aircraft elements, and the rules of execution for the drawings of the general appearance of the aircraft and the common device of its units were all used.

The following aircraft have been chosen to represent this class in the statistics collection process:

- a.B737-800
- b.B737-900ER
- c.A320-200
- d.AN-158
- e. TU-214

1.1.3. Gathering and processing of the statistical data, their analysis

For the compilation of the statistical data, it is necessary to use the data of aircrafts similar to the designed aircraft. The engines, performance characteristics, maintenance requirements, and number of passengers or

mass of cargo carried should all be identical throughout all aircraft prototypes.

To obtain the best design solutions while accounting for various computational constraints and limitations, physical and mathematical models are commonly used in modern engineering design. This is done by employing a variety of computer programs. This project uses calculations as well as a design strategy based on data from current aircraft statistics. The gathering and analysis of statistical data, which takes into account:

- ❖ The types of aircraft required by modern aviation;
- ❖ The tasks they perform;
- ❖ Flight technical characteristics;
- ❖ Means of achieving these qualities: the applicable schemes of aircraft, geometric and mass parameters, power plant.

To identify patterns and potential directions for the development of the aircraft type, quantitative and qualitative modifications to the aircraft, the development of its intended use, and production and operational conditions.

Five aircraft prototypes are described briefly below.

a.B737-800

In September 1994, Boeing began design work on the Boeing 737-800, the second in the new 737 subfamily, which is a 2.8 m long 737-800 aircraft. It has the same passenger capacity as the 737-400. Its design uses all those technical solutions that are used on the original variant 737-700. The aircraft is designed to carry 180-200 passengers. As a power plant, it is planned to use two CFM56-7B turbofan engines with a thrust of 12950 kgf each, figure 1.1.

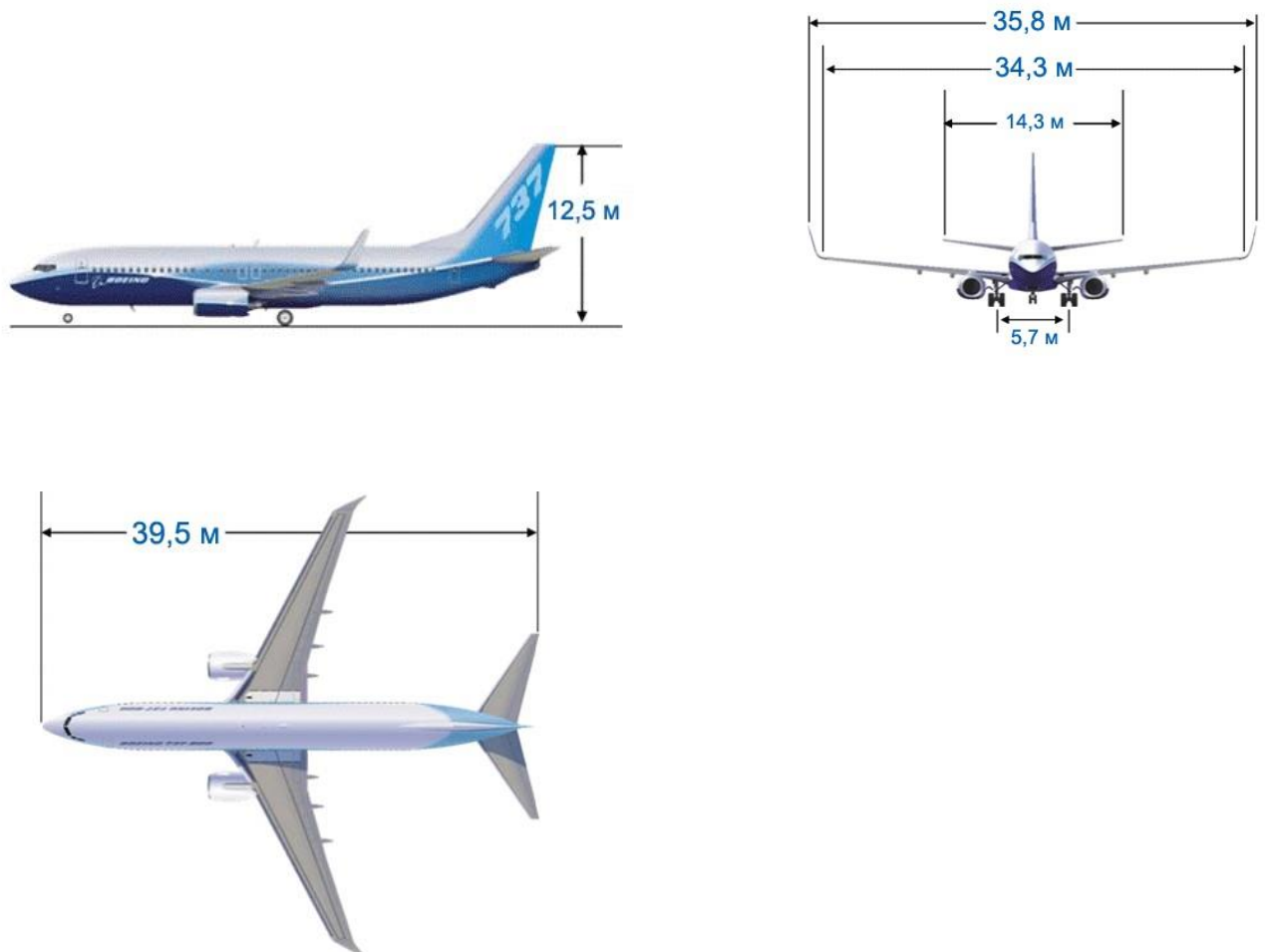


Figure 1.1 - Scheme of the B737-800

b.B737-900ER

Liner 737-900 is similar to 737-800, but has a fuselage extended by 2.8 meters. It seats more passengers than the Boeing 707 and is in the same class as the Boeing 757. For more successful competition with Airbuses, the Boeing 737-900 model was developed - the longest aircraft in the family, but noticeably smaller than the Airbus. New double-slotted flaps were used in the flight control system, one section of slats and spoilers was added. landing gear redesigned, taller than the 737 Classic and also reinforced depending on the takeoff weight. Since 2008, it has become possible to install new carbon brakes, which have a lower mass and a longer resource, figure 1.2.

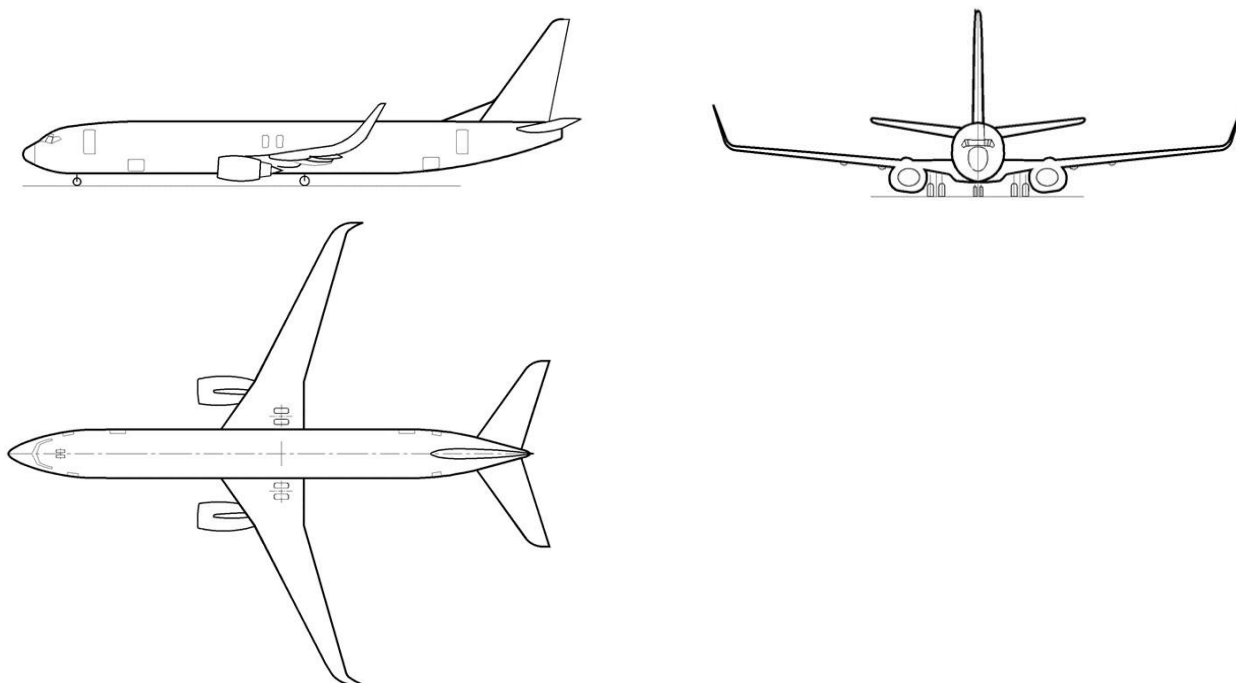


Figure 1.2 - Scheme of the B737-900ER

c.A320-200

The A320 is the main variant, with Airbus producing the A320-200 with winglets starting with the 22nd A320. It features winglets on the wingtips and enlarged fuel tanks for increased cruising range. The A320-200 can carry 150 passengers and has a cruising range of about 2,900 nautical miles. It uses two CFM International CFM56-5 or International Aero Engines V2500 engines with a thrust of 25,500 to 27,000 pounds, figure 1.3.

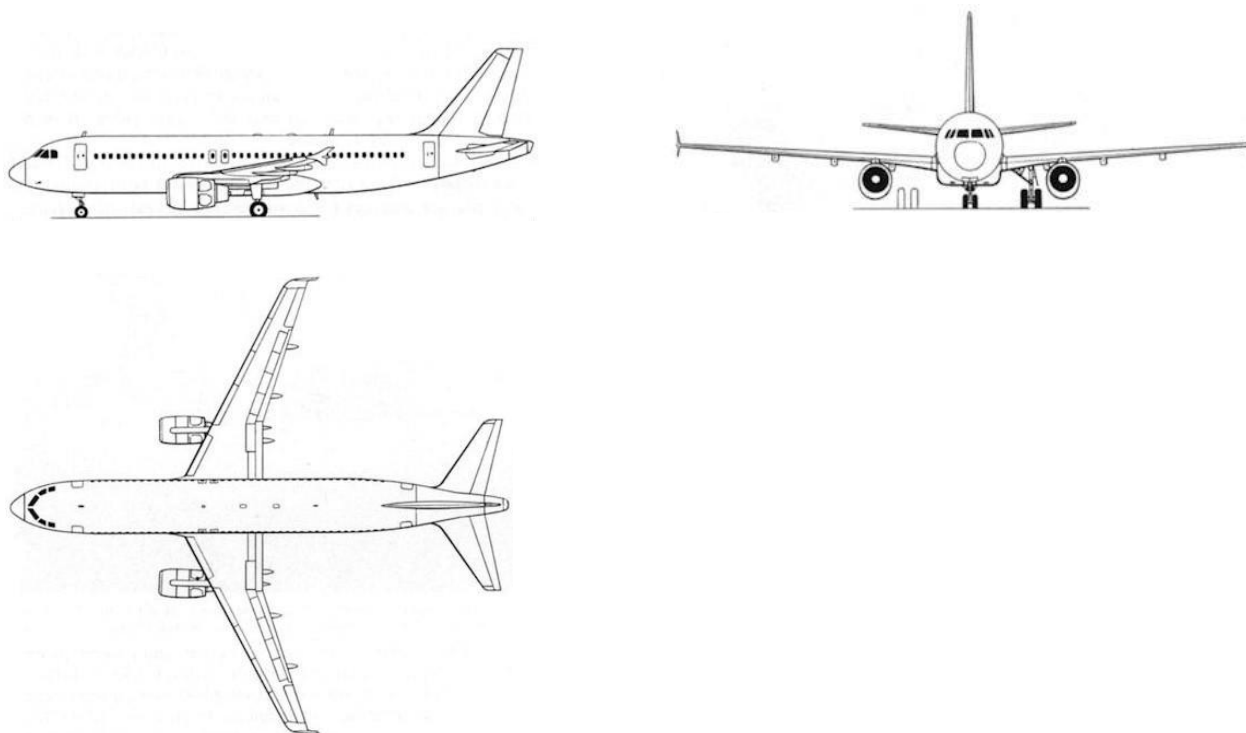


Figure 1.3 - Scheme of the A320-200

d.AN-158

An-158 is a continuation of the An-148 lineup. Due to the increased number of seats per passenger kilometer, the performance of the aircraft has improved by 15-18%. At the same time, in terms of fuel efficiency, the new An is somewhat superior to the similarly dimensioned Sukhoi Superjet 100 due to a better wing and more economical than SaM.146 engines D-436-148. According to preliminary estimates, in cruising flight mode with a Mach number of 0.7-0.75, the An-158 has an aerodynamic quality of 0.5-1 unit higher than the SSJ100, and its power plant consumes 3-5% less fuel. This happens because the An-158 has a larger wing span and elongation with a slightly smaller fuselage diameter. At the same time, the progressive three-shaft scheme D-436 has a number of advantages over the simpler two-shaft SaM. 146,figure 1.4.



Figure 1.4 - Scheme of the AN-158

e. TU-214

First released in 1983, the Tu-214 was developed to replace the Tu-154 and Il-62. The first flight on January 2, 1989 was powered by a PS-90AT engine. Originally used as a transport aircraft, it was first used as a passenger aircraft by Russian Vnukovo Airlines on February 23, 1996. A total of 17 of the aircraft were delivered. It adopts swept-back lower monoplane with wing tilt; two Aviadvigatel PS-90A or Rolls-Royce RB 211-535 turbofan engines are suspended under the wing; swept-back vertical tail and lower horizontal tail, figure 1.5.



Figure 1.5 - Scheme of the TU-214

1.2. Technical Data

Table 1.1 - Technical Data

NO	Name of Aircraft	FLIGHT DATA					MASS DATA				
		V_{max} , km/h	V_{CR} , km/h	H_{sc} , m	L, km	L_P , m	M_{0max} , kg	M_L , kg	M_{EM} , kg	M_C , kg	n_{pas}
1	B737-800	876	828	12500	5665	2450	79010	66361	41413	20540	189
2	B737-900ER	876	823	12500	4996	2450	85130	66361	44676	20240	215
3	A320-200	871	828	12000	5950	2090	78000	66000	42600		186
4	AN-158		800-870	12200	2100-4400	1900	43700			5000	86-99
5	TU-214	900	810-850	12100	4340	2030	110750	93000	59000		210
6	My airliner	870	830	12500	5600	2500	739600	66400	45000	25000	200

Continuation of table 1.1

NO	Name of Aircraft	Data of a power-plant					Geometrical Data						
		type	n_{EN}	$P_0, (K/N)$	$m_{EN}, k/g$	S, m^2	L, m	$\chi_{0.25}, ^\circ$	λ	λ_ϕ	\bar{S}_{HS}	\bar{S}_{VS}	
1	B737-800	Turbo fan,2	2	121	2370	124.6	35.7	25.02	9.45	10.21	0.26	0.21	
2	B737-900ER	Turbo fan,2	2	117	2370	124.6	35.7	25.02	9.45	10.91	0.26	0.21	
3	A320-200	Turbo fan,2	2	147	2467	122.6	34.1	25		10.2			
4	AN-158	Turbo fan,2	2	67	1400	87.32	28.91			15.55			
5	TU-214	Turbo fan,2	2	158.2	2950	184.2	41.8			12.1			
6	My airline	Turbo fan,2	2	130	2370	111.72	32.492	25.02	9.45	10	0.26	0.21	

End of table 1.1

NO	Name of Air	Derivative Parameters					Landing		Geometrical Data									
		P ₀ (N/	t ₀	γ _{EN}	K _C	Wheel	Track,	η	C̄, %	b _f	δ _f , °	λ _{HS}	X _{HS} ,	X _{VS}	C̄	η _{VS}	η _{HS}	
1	B7 37-800	621 4.2 7	0.0 080 2	0.0 196	0.2 6	15. 6	5.7 15	6.3	12. 5	0.1 26	35	6.1 4	1.9 1	30	35	10. 8	0.2 01	3.6 5
2	B7 37-900	669 5.6 2	0.0 080 3	0.0 203	0.2 4	15. 6	5.7 15	6.3	12. 5	0.1 26	35	6.1 4	1.9 1	30	35	10. 8	0.2 01	3.6 5
3	A3 20-200	623 4.9 1	0.0 081 6	0.0 168		12. 64	4.8 25											
4	AN - 158	490 4.4 9	0.0 114 5	0.0 209	0.1 1													
5	TU - 214	589 2.2 4	0.0 054 3	0.0 186														
6	Projected		0.0 18	0.0 201	0.2 3	12. 652	5.7 15	6.3	12. 5	0.1 26	35	6.1 6	1.9 1	30	35	10. 8	0.2 03	3.6 9

1.2.1. Aircraft tactical-technical requirements development

It is feasible to develop Tactical and Technical Requirements (TTR) for the developed aircraft based on the analysis of statistical data in table 1.2.

- i. The purpose of the aircraft.
- ii. Flight characteristics.
- iii. Requirements of the equipment.
- iv. Requirements for the crew.
- v. Requirements for the power plant.
- vi. Requirements for strength, rigidity and reliability.

Table 1.2 – Tactical and Technical Requirements

Range (km)	Passenger	Take-off distance (km)	Cruise speed (km/h)	Cruise Altitude (km)	Number of the crew member
5600	160	1.95	830	11.9	4

1.2.2. Selection and justification of the aircraft layout

An aircraft's aerodynamic configuration is typically described as a system of the load-bearing surfaces' relative positions (the wings and stabilizers), sizes, and shapes. The method of aircraft longitudinal trimming is the main feature of the aircraft configuration.

The compensation of all forces and moments acting on an aircraft relative to its longitudinal axis is known as longitudinal trimming. There

are four different balancing configurations for the aircraft based on how the stabilizers are arranged in relation to the wings. The majority of contemporary airplanes have the "normal" classical configuration.

Advantages of the Normal configuration are:

- 1 The wings are in the unadulterated, undisturbed airflow and is not shadowed by stabilizers;
- 2 The nose section of the fuselage is short and does not cause a destabilizing moment relative to the vertical axis, allowing for the reduction of the area and mass of vertical stabilizer;
- 3 The crew has superior observation of the front semi-sphere.

The disadvantage of the Normal configuration is:

- 1 The horizontal stabilizer (HS) is caught up by the skewed airflow disturbed by wing; this reduces its efficiency, causing the necessity of an increase of its area and mass, and if HS position is shifted beyond turbulence zone upwards, downwards or on the vertical stabilizer (VS) the mass of the VS and fuselage increases;

One of the key factors taken into consideration when constructing an aircraft is Cruise speed (V_{cr}). This is a mid-range transport. In this case, I have to install powerful engines to get a high level of thrust. According to the projected values from my table of statistical data, I selected the cruise speed as 839 km, this also depends on the fuel consumption and the

optimal performance of the engines and the aircraft. In modern aircrafts, they have automatic controls and navigation tools/systems and because of this development the number of crew members in these aircrafts are less. In most mid-range aircrafts, the crew are about 4 or 6 including pilots and stewardesses. Furthermore, in this project I chose 5 crew members for my new aircraft. $N_{\text{crew}} = 4$. The aircraft's technical data and parameters are shown below in Table 1.3.

Table 1.3 – Basic Parameters of the Airplane

λ	$\chi_{0.25}$	η	\bar{C}	\bar{b}_{FL}	\bar{S}_{AL}	λ_F	D_F, m
9.45	25.02 ⁰	6.3	10.8	0.25	0.035	10.5	3.74

Continuation of table 1.3

\bar{S}_{HS}	\bar{S}_{VS}	λ_{HS}	λ_{VS}	$\chi_{HS,0.25}$	$\chi_{VS,0.25}$	\bar{C}_{HS}	\bar{C}_{VS}	η_{HS}	η_{VS}
0.26	0.21	6.16	1.91	30 ⁰	35 ⁰	0.1	0.12	4	1.5

1.2.3. Calculation of aircraft zero approximation take-off mass

This formula determines the take-off mass of the aircraft at zero approximation. Formula (1.1) mentioned below. The required parameters are gotten from the table of statistical data.

$$m_0 = \frac{m_{OP} + m_C}{1 - (\bar{m}_{airfr} + \bar{m}_{PP} + \bar{m}_{EQ} + \bar{m}_F)} \quad (1.1)$$

Where m_0 – take-off mass of the airplane in zero approximation;

m_C – mass of payload;

m_{OP} – mass of operational load/crew;

\bar{m}_{air} – mass ratio of the airplane structure;

m_{PP} – mass ratio of the power-plant;

m_{EQ} – mass ratio of the equipment;

m_F – mass ratio of fuel.

Mass of payload m_C is calculated using 120kg as the mass of one passenger with luggage. Consequently, the mass of our airplane's payload is calculated by the equation 1.2 below:

$$m_C = 120 \times \text{number of passengers} \quad (1.2)$$

$$m_C = 120 \times 160 = 18960 \text{ kg}, m_C = 20000 \text{ kg}$$

Mass of operational load/crew is determined taking the mass of each crewmember to be 80 kg, and is calculated by the equation:

$$m_{CR} = 80 \times n_{CR} \quad (1.3)$$

$$m_{CR} = 80 \times 6 = 480 \text{ kg}$$

Where n_{CR} – number of crew members (pilots and stewards) are derived from the analysis of statistical data or the aforementioned recommendations.

Value of mass ratio of fuel m_F is determined by the formula (1.4) below:

$$m_F = 1.1 \left(1 - e^{-(L \cdot C_{const}) / (V_{cruise} \cdot K_{max})} \right) \quad (1.4)$$

$$m_F = 0.52$$

Where L – flight range, km (5600 km);

V_{CR} – cruising speed of flight, km/h (830 km/h)

For aircraft powered by turbojet engines, factors **a** and **b** have values: $a = 0.05$, $b = 0.04$

Mass ratio of structure m_{airf} , power plant m_{PP} , equipment m_{EQ} for the projected aircraft were given as follows:

$$m_{airf} = 0.24$$

$$m_{pp} = 0.05$$

$$m_{eq} = 0.09$$

$$m_f = 0.52$$

Following the determination of the mass of the passengers and crew, the mass ratio of the structure, power plant, and equipment were selected, as well as the mass ratio of fuel based on the data presented. The prior formula (1.1) is then used to estimate the take-off mass of the aircraft in zero approximation.

$$m_0 = \frac{m_{OP} + m_C}{1 - (\bar{m}_{airf} + \bar{m}_{PP} + \bar{m}_{EQ} + \bar{m}_F)}$$

$$m_0 = (480 + 20000)/1 - (0.24 + 0.05 + 0.09 + 0.52)$$

$$m_0 = 204800 \text{Kg.}$$

1.2.4. Calculation of the structural mass of the main aircraft assemblies, power plant mass, fuel mass, mass of the equipment and controls

Using values from the statistical data shown in table 1.1, the mass of the wings, fuselage, tail unit, and landing gear is calculated . This table displays the mass ratio of the aircraft units as a share of the total structural mass. m_{air} .

Values of unit mass are found by the formula

$$m_i = \bar{m}_i \cdot \bar{m}_0 \quad (1.5)$$

The total sum of the unit mass ratio m_i for designed airplane must be equal to 1, that is $\sum \bar{m}_i = 1$

Mass of structure

$$M_{airf} = m_{airf} * m_0 = 0.29 * 74461.5 = 49152 \text{ kg.}$$

Mass of power plant

$$M_{pp} = m_{pp} * m_0 = 0.10 * 74461.5 = 10240 \text{ kg.}$$

Mass of equipment

$$M_{eq} = m_{eq} * m_0 = 0.12 * 74461.5 = 18432 \text{ kg.}$$

Mass of fuel

$$M_f = m_f * m_0 = 0.52 * 204800 = 106496 \text{ kg.}$$

For wing, fuselage, tail unit and landing gear masses I multiplied the ratio of the structural mass of the aircraft to the structural mass.

Chosen mass ratio of the aircraft units

- mass ratio of wing $\bar{m}_w = 0.396$
- mass ratio of the fuselage $\bar{m}_{fus} = 0.351$
- mass ratio of tail-unit $\bar{m}_{TU} = 0.069$
- mass ratio of landing gear $\bar{m}_{LG} = 0.184$

Thus, the respective masses are calculated accordingly:

$$\text{Mass of wing } m_W = \bar{m}_w \times m_{aifr} = 0.396 \times 49152 = 19464.2 \text{ kg.}$$

$$\text{Mass of the fuselage } m_{FUS} = \bar{m}_{fus} \times m_{aifr} = 0.351 * 49152 = 17252.4 \text{ kg.}$$

$$\text{Mass of tail-unit } m_{TU} = \bar{m}_{tu} \times m_{aifr} = 0.069 * 49152 = 3391.5 \text{ kg}$$

$$\text{Mass of landing gear } m_{LG} = \bar{m}_{lg} \times m_{aifr} = 0.184 * 49152 = 9044 \text{ kg.}$$

Table 1.4 – The mass values of the aircraft units

m_0 kg	m_C kg	m_{CR} kg	m_F kg	m_{PP} kg	m_{EQ} kg	m_{aifr} , kg			
						m_W kg	m_{FUS} kg	m_{TU} kg	m_{LG} kg
20480	2000	480	1064	10240	18432	19464.2	17252.4	3391.5	9044
0	0		96			49152			

1.2.5. Engine selection and its characteristics

Further, it is necessary to determined starting thrust of the engine P_0 .

It is determined on the collected statistical values of starting thrust-to-weight ratio t_0 .

Then it is possible to find starting total thrust of engines,

$$P_0 = t_0 m_0 g \quad (1.6)$$

Where $g = 9.8 \text{ m/s}^2$,

$t_0 = 0.018$ (from statistical data)

$$P_0 = 0.018 * 204800 * 9.8 = 36126.72 \text{ N}$$

Further starting thrust of one engine can be determined on the basis of engines number.

$$P_{o1} = P_0 / n \quad (1.7)$$

$$P_{o1} = 36126.72 / 2 = 18063.36 \text{ N}$$

Approximately equal to 18 kN. On this basis I have chosen The CFM 56-7B18 engines. having a thrust of 86.7 kN.

A copy of the general view of the engine is also provided in the figure 1.6 below:



Figure 1.6 – Scheme of CFM 56-7B18 Engine

The engine specifications are shown in the table 1.5 below;

Table 1.5 – Engine specifications

Model	CFM 56-7B18
Type	Turbofan engine
Length	250.8 cm (98.7 in)
Fan diameter	61 in (155 cm)
Weight	5,216 lb (2,370 kg)
Compressor	Axial flow, 1 fan, 3 LP, 9 HP
Combustor	Annular (double annular for -5B/2 and -7B/2 "DAC")
Turbine	Axial flow, 1 HP, 4 LP
Take-off Thrust	91.63–121.43 kN 20,600–27,300 lbf
Thrust-to-weight ratio	3.84-5
Bypass ratio	5.5
Overall Pressure ratio	32.7

1.2.6. Determination of the basic geometrical parameters of the aircraft assemblies (fuselage, tail units, landing gear). Calculation of its center-of-gravity position. General view development.

Fuselage Parameters

The size and mass of the payload are often what determines the shape and size of subsonic aircrafts. Depending on the size and range of the aircraft, the payload configuration may change.

The main parameters needed to start the construction of the fuselage section are:

$$L_F(\text{Overall fuselage length}) = \lambda_F * D_F = 10 \times 4 = 40 \text{ m ;}$$

$$L_N(\text{Fuselage nose length}) = \lambda_N * D_F = 2 \times 4 = 8 \text{ m ;}$$

$$L_T(\text{Fuselage rear length}) = \lambda_T * D_F = 3 \times 4 = 12 \text{ m ;}$$

Where $\lambda_F, \lambda_N, \lambda_T$ are the aspect ratio of fuselage, nose, and tail respectively.

Tail-unit parameters

The horizontal stabilizer and vertical stabilizer make up an aircraft's tail unit. The geometric calculations used for the construction of the tail-unit are similar to those used to construct the wings.

The distance between the center of mass of the aircraft and the center of pressure of its horizontal tail unit L_{HS} for the “normal” configuration is determined according to recommendations which depends on the values from the statistical data.

The distance between the vertical tail unit's center of pressure and the aircraft's center of mass L_{VS} in zero approximation may be considered to be equal to the distance of horizontal tail-unit, where $L_{VS} = L_{HS}$.

Horizontal tail unit

The surface area the horizontal stabilizer is gotten from the formula (1.16):

$$S_{HS} = \bar{S}_{HS} * S$$

(1.8)

$$S_{HS} = 0.26 \times 111.72$$

$$S_{HS} = 29.05 \text{ m}^2;$$

Where \bar{S}_{HS} - the ratio of surface area of the horizontal stabilizer to the wing's area.

The length of the Horizontal stabilizer is equal to

$$L_{HS} = \sqrt{\lambda_{HS} * S_{HS}} \quad (1.9)$$

$$L_{HS} = \sqrt{6.16 * 29.05} = 13.38 \text{ m};$$

Where the value of λ_{HS} is taken from table 1.4 ($\lambda_{HS} = 6.16$).

Chords of Horizontal tail unit

Root (on axis of airplane symmetry) b_0_{HS} and tip b_k_{HS} chords are determined using the values S_{HS} , η_{HS} , L_{HS} and are calculated using the formulas (1.10) and (1.11) below:

$$b_{0_{HS}} = (S_{HS} / L_{HS}) * (2\eta_{HS} / (\eta_{HS} + 1))$$

(1.10)

$$b_{0_{HS}} = (29.05/13.38) * (2 * 3.69 / (3.69 + 1)) = 3.61 \text{ m}$$

$$b_{k_{HS}} = b_{0_{HS}} / \eta_{HS} = 3.61 / 3.69$$

(1.11)

$$b_{k_{HS}} = 0.73 \text{ m}$$

Where value $\eta_{HS} = 3.69$ and is taken from table (1.3).

Mean aerodynamic chord (MAC) of HS is calculated by the formula (1.12).

$$b_{AHS} = \left\{ \frac{2}{3} * b_{0HS} * (\eta_{HS}^2 + \eta_{HS} + 1) \right\} / \left\{ \eta_{HS} (\eta_{HS} + 1) \right\} \quad (1.12)$$

$$b_{AHS} = \left\{ \frac{2}{3} * b_{0HS} * (\eta_{HS}^2 + \eta_{HS} + 1) \right\} / \left\{ \eta_{HS} (\eta_{HS} + 1) \right\} = \left\{ \frac{2}{3} * 3.61 * (3.69^2 + 3.69 + 1) \right\} / \left\{ 3.69 * (3.69 + 1) \right\} = 3.09 \text{ m}$$

Coordinate of MAC along Horizontal stabilizer is determined by the relation (1.13) below

$$Z_{AHS} = (L_{HS} / 6) * (\eta_{HS} + 2) / (\eta_{HS} + 1) = (13.38 / 6) * (3.69 + 2) / (3.69 + 1) \quad (1.13)$$

$$Z_{AHS} = 2.71 \text{ m}$$

Coordinate of MAC nose along an axis θx

$$X_{AHS} = Z_{AHS} * \tan \chi_{LE(HS)} \quad (1.14)$$

$\chi_{LE} = 30^\circ$ (sweep angle of the horizontal stabilizer's leading edge)

taken from table 1.3.

$$\tan \chi_{LE(HS)} = \tan \chi_{HS} + (\eta_{HS} - 1) / \left\{ \lambda_{HS} (\eta_{HS} + 1) \right\} = \tan(30^\circ) + (3.69 - 1) / \left\{ 6.16 * (3.69 + 1) \right\} = 0.671$$

$$\tan \chi_{LE(HS)} = 0.671 \text{ thus, } X_{AHS} = 2.71 * 0.671 = 1.82 \text{ m}$$

Vertical tail unit

The surface area the vertical stabilizer is calculated using the formula (1.15):

$$S_{VS} = \bar{S}_{VS} * S$$

$$(1.15)$$

$$S_{VS} = 0.21 * 111.72$$

$$S_{VS} = 23.46 \text{ m}^2;$$

Where $\bar{S}_{VS} = 0.21$ - the ratio of surface area of the vertical stabilizer to the wing's area.

Length of Vertical stabilizer is equal to

$$L_{VS} = \sqrt{\lambda_{vs} * S_{vs}}$$

(1.16)

$$L_{VS} = \sqrt{1.91 * 23.46};$$

$$L_{VS} = 6.69 \text{ m}$$

Where the value of λ_{VS} is taken from table 1.3.

Chords of Vertical Stabilizer

Root (on axis of airplane symmetry) b_0 VS and tip b_k VS chords are determined proceeding from the values S_{VS} , η_{VS} , L_{VS} ;

$$b_{0VS} = (S_{VS} / L_{VS}) * (2*\eta_{VS} / \eta_{VS} + 1) \quad (1.17)$$

$$b_{0VS} = 3.37 \text{ m}$$

$$b_{kVS} = b_{0VS} / \eta_{VS} \quad (1.18)$$

$$b_{kVS} = 3.37 / 0.203$$

$$b_{kVS} = 0.91 \text{ m}$$

Where $\eta_{VS} = 0.203$ (taken from table 1.3);

The Mean aerodynamic chord (MAC) of Vertical stabilizer is

$$b_{AVS} = \{ (2/3) * b_{0VS} * (\eta_{VS}^2 + \eta_{VS} + 1) \} / \{ \eta_{VS} (\eta_{VS} + 1) \} \quad (1.19)$$

$$b_{AVS} = 2.38 \text{ m}$$

The Co-ordinate of MAC along a Vertical stabilizer is

$$Z_{AVS} = (L_{VS} / 3) * (\eta_{VS} + 2) / (\eta_{VS} + 1)$$

$$Z_{AVS} = 2.71 \text{ m}$$

Co-ordinate of MAC nose along an axis $0x$

$$X_{AVS} = Z_{AVS} * \tan \chi_{LE (VS)} \quad (1.20)$$

$\chi_{LE} = 35^0$ (sweep angle of the vertical stabilizer's leading edge) is taken from table 1.3.

$$\tan \chi_{LE (VS)} = \tan \chi_{VS} + (\eta_{VS} - 1) / \{ \lambda_{VS} (\eta_{VS} + 1) \} = \tan(35^0) + (0.203 - 1) / \{ 1.91 * (0.203 + 1) \} = 0.35$$

$$\tan \chi_{LE (VS)} = 0.35,$$

$$\text{thus, } X_{AVS} = 2.68 * 0.35 = 5.64 \text{ m}$$

Determination of the position of center of mass of the airplane

Position of the airplane's center of mass is determined in relation to the nose part of the wing's mean aerodynamic chord (MAC).

The recommended distance for the center of mass (point 0) from nose part of the mean aerodynamic chord (X_m) has these values for the airplanes with swept wing

$$X_m = (0.26 \dots 0.30) * b_A = 0.26 * 4.04 = 1.05 \text{ m}$$

$$\text{Swept wing } \chi (30^0 \dots 60^0)$$

On the basis of the chosen value, distance for the airplane's center of mass from nose point of mean aerodynamic chord along the axis can be determined.

Distance from the airplane center of mass up to the horizontal tail-unit center of pressure (L_{HS})

$$L_{HS} = (2.5 \dots 3.5) * b_A \quad (1.21)$$

$$L_{HS} = 3.5 \times 4.04$$

$$L_{HS} = 14.14 \text{ m}$$

Determination of Landing gear parameters:

The following are parameters of three strut landing gear;

- 1 Landing gear wheelbase, b
- 2 Landing gear wheel track, B
- 3 Offset, e (the horizontal distance between the center of gravity and main landing gear).
- 4 Height of landing gear, h
- 5 Height of airplane's center of mass, H

Derivatives of these parameters will be;

- 1 Angle of offset for wheels of main struts, γ
- 2 Angle of overturning, ϕ (angle of a touchdown of a fuselage tail section with runway surface).

Landing gear wheelbase b depends on fuselage length:

$$b = (0.30 \dots 0.40) * L_F \quad (1.22)$$

$$b = 0.40 * 40$$

$$b = 16\text{m}$$

Offset

$$e = (0.12 \dots 0.06) * b \quad (1.23)$$

$$e = 0.08 * 16$$

$$e = 1.28 \text{ m}$$

Note; At a high value of *the offset* of the nose gear, rising off is complicated during attainment of the aircraft's take-off angle of attack. In this case, lift-off will occur at a higher speed, hence the length of the take-off run will increase.

Reduction of the dimension of *the offset* will provide easier rising off of the nose gear. However, at a low height rolling over the aircraft on tail is possible landing the aircraft center of mass can go behind the point of support of the main wheels.

If the aircraft structure is such that its center of mass can be displaced behind the support line of the main wheels then in order to prevent lowering the aircraft's tail section it is necessary to provide the auxiliary tail support.

The distance between the nose strut and the center of mass an is selected so that the loading on the nose strut during aircraft parking would be equivalent to around 6–12% of the mass of the aircraft.

$$\text{Thus, } a = (0.88 \dots 0.94) * b \quad (1.24)$$

$$a = 0.92 * 16$$

$$a = 14.72 \text{ m}$$

The sum of offset and nose strut and center of mass must be equal to the landing gear wheelbase.

$$b = a + e \quad (1.25)$$

$$16 = 14.72 + 1.28$$

The h - height of the landing gear is determined from the condition of providing minimum gap 200...250 mm between runway surface and the airplane structure with separate and simultaneous compression of tires and shock absorbers. This gap must be determined for aircraft landing with rolling.

Calculation of angle of touch down:

$$\Phi = \alpha_{\max} - \alpha_w - \psi \quad (1.26)$$

$$\Phi = 12^\circ - 0^\circ - 0^\circ = 12^\circ$$

Where $\alpha_w = (0 \dots 4)^\circ = 0$ (angle between a wing chord and longitudinal axis of fuselage), $\psi = 0$ (static ground (parking angle) in zero approximation it is $\psi = 0$), $\alpha_{\max} = \text{maximum angle of attack} = 12^\circ$.

Angle of main wheel offset γ

$$\gamma = \Phi + (2\sigma) \quad (1.27)$$

$$\gamma = 12^\circ + 2^\circ = 14^\circ$$

In conjunction with the center of mass e and angle γ the greater the value e the greater the front tail support loads and the more difficult to take off a front support during take-off. But the lesser the e , the γ reduces.

Calculation of height of airplane center of mass (H)

$$H = \frac{e}{\tan(\gamma)} \quad (1.28)$$

$$H = 1.28 / \tan(14) = 5.13 \text{ m}$$

Calculation of the height of landing gear

$$h = H - \frac{D_F}{2} \quad (1.29)$$

$$h = 5.13 - (4 / 2)$$

$$h = 3.13 \text{ m}$$

Calculation of distance between two main landing gears (B)

$$2H \leq B < 15 \text{ m}$$

$$2H = 10.26 \text{ m}$$

side friction coefficient $\mu = 0.85$

$$B = \frac{2 * H * b * \mu}{\sqrt{a^2 - H^2 * \mu^2}} \geq 2H \quad (1.30)$$

$$B = 11.57 \text{ m}$$

10.6 m < 11.57 m < 15 m, the condition is satisfied.

1.2.7. Selection, justification, development and reconciliation of aircraft load-carrying structure

Determination of the General arrangement of Airplane Units

Such essential rules as the following must be taken into consideration while determining the general arrangement of airplane units

- The airframe structure of an airplane should have the least mass possible under the given circumstances, which is accomplished by rationally transferring loads to structural elements with necessary rigidity.
- Structure must be adaptable, allowing for the application of the most straightforward and logical manufacturing techniques.
- Structure must be highly survivable, i.e. ability to withstand operational loads even if some of its individual members fail partially, and meet fatigue strength criteria.
- Structure must provide the greatest convenience in operation of the airplane due to rational arrangement of hatches and maintenance breaks in units for access to the power plant, equipment, arms, etc.

All of these tasks need the use of statistical data primarily detailing the general arrangements of the airplane units. The airplane's principal structural parts are shown in a circuit of coordination that includes the position of spars, the false spars of a wing and tail unit, and the

attachment fittings for the engines (nacelles) and landing gear struts to strong ribs or frames.

Load-carrying Structure of Wing

The choice of load-carrying structures for wing is determined by;

- Wing configuration - Presence of hatches for servicing the equipment units in wings, fuel tanks inside wings, landing gear struts and wheels, etc.
- Fuselage configuration - presence of sufficient volumes for the wing center section in fuselage.
- Rigidity requirements.

Determination of Load-carrying Structure of a Wing

For an accurate choice of the load-carrying structure of wing, two criteria may be used.

A) Concept of Conventional Spar

B) Criterion of Load Moment Intensity

Through their respective equations and techniques, these two methodologies are used in the calculation of the load-carrying structure. I considered the conventional spar approach when I calculated the load-bearing structure. This does not imply that the load-carrying structure must be satisfactory; rather, it is decided by particular calculating techniques. Aerodynamic, dependability, manufacturing (technology) and operational requirements still exist.

It is possible to develop the solution for a wing's load-carrying structure by taking into account a broad range of requirements.

Concept of Conventional Spar (Spar Ratio)

$$\delta_y = \frac{(p_0 s z_A - 2m_c g z_i - m_w g z_A) n^p}{0.96 * \bar{c} * b_0^2 * \sigma_p}$$

(1.31)

Where P_0 wing loading = 1796.5 N/m²

S = wing area = 111.72 m²

Z_a = coordinate of mean aerodynamic chord of a wing span wise =

6.16m

$m_i = m_{eng}$ = mass of engine = 2,370 kg

Z_i = engine distance from center = 1.25

\bar{c} = Airfoil thickness ratio = 0.125

b_0 = 5.93 m

n^p = g- load (choosing from recommended table 3) = 3

σ_p = Allowable stress of the using materials (Chosen from standard metal)

σ_p = 330 Mpa (Aluminium alloy)

m_w = mass of wing = 19464.2 kg

δ_y = 7.03 mm

Since the value is greater than 3mm, I am going to use the torsion-box type of wing.

Criterion of Load Moment Intensity:

$$\frac{M}{H^3} = \frac{[(p_o \cdot s - m \cdot g)Z_A]n^P}{1.03(c \cdot b_o)^3}$$

(1.32)

Where $n = 3$

$$f = 1.5$$

$$S_{OTC} = 8.56 \text{ m}^2$$

$$S = 137.74 \text{ m}^2$$

$$M_0 = 74461.5 \text{ kg}$$

$$M_W = 8551 \text{ kg}$$

$$Z_{OTC} = 3.42 \text{ m}$$

$$M_{\text{fuel}} = 531 \text{ kg}$$

$$Z_{\text{fuel}} = 2.92 \text{ m}$$

$$\bar{c} = \text{Airfoil thickness ratio} = 0.125$$

$$b = 2.4 \text{ m}$$

$$M / H^3 = 51 \text{ MPa}$$

Where M - bending moment, Nm; H - design thickness of airfoil section, m;

$$H = 0.8 H_{\text{max}},$$

H_{max} - maximum thickness of wing airfoil section in its root wing portion, m.

If the size of the load moment intensity does not exceed 10... 15 MPa, in this case spar-type wing is more favorable in the mass criterion.

If relation M/H^3 is more 10... 15 MPa, monoblock-type (stressed-skin-type) or torsion-box-type wing will have advantage.

Determination of distance between Ribs and Stringers

The distance between the ribs is chosen depending on thicknesses and sizes of stringer sections. Very short distances are disadvantageous owing to plenty of rivets. It results in quality deterioration of a wing surface, complication of its manufacturing process, appearance of stress increase in large quantity.

As the wing of designed aircraft does have stringers, therefore the distance between ribs is $a = 400$ mm.

The distance between stringers is considered to be $b_{str} = 250$ mm according to the regulations.



Figure 1.7 – Wing Load-Carrying Structure

Load carrying structure for fuselage

The fuselage load-carrying structure is of the semi monocoque type, it consists of skin, stringers and frames. The distance between frames

depends on the thickness of the skin and from the regulations, the chosen distance $a = 400\text{mm}$.

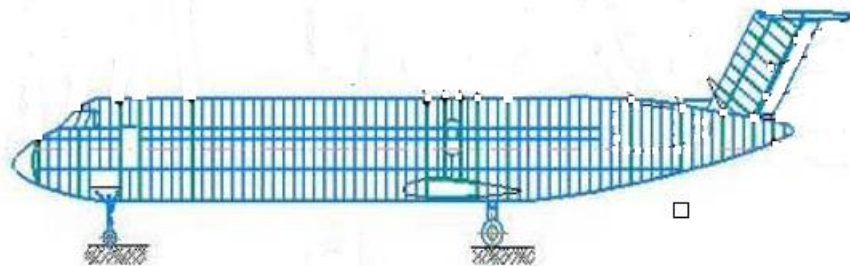


Figure 1.8 – Fuselage Load-Carrying Structure

Load-Carrying Structures of Vertical Tail Unit

As previously done in the wing section unit, I have to consider two parts for the vertical tail section as well. One is the root tail chord and the other is the tip chord of the vertical fin.

The distance between ribs $a = 400\text{mm}$.

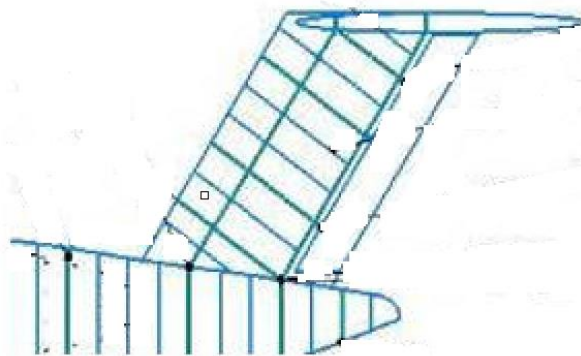


Figure1.9 – Vertical tail Load-Carrying Structure

Load-Carrying Structures of horizontal Tail Unit

Just as the vertical tail unit, I have to consider two parts for the horizontal tail section also. One is the root tail chord and another on the tip chord.

The distance between ribs $a = 400\text{mm}$.

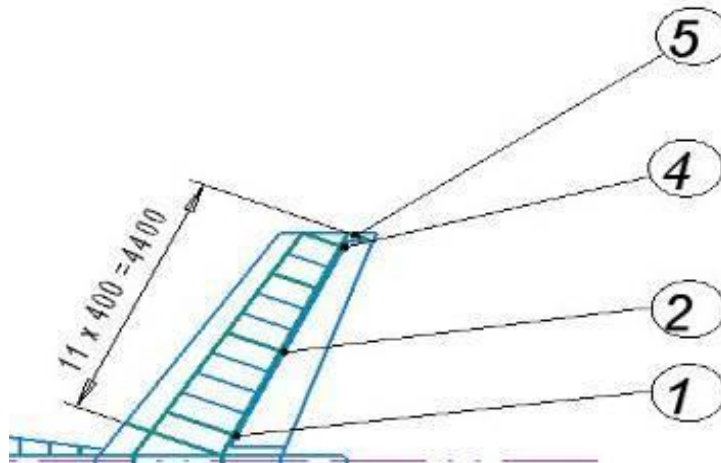


Figure 1.10 – Horizontal tail load-carrying structure

Landing gear:

The under carriage or landing gear is the structure (mostly wheels, but sometimes skids, floats or other types of elements) that supports an aircraft on the ground and enables the aircraft during taxiing, take-off and landing. In my case I used the nose Landing gear, which can be retracted forward, and the main landing gear, which can be retracted back into wing's structure[2]. The load-carrying structures of the landing gear should ensure:

- The least possible mass of the landing gear,
- The least possible volume of the landing gear in retracted position,

- And a simple kinematic structure for its mechanisms of extension and retraction.

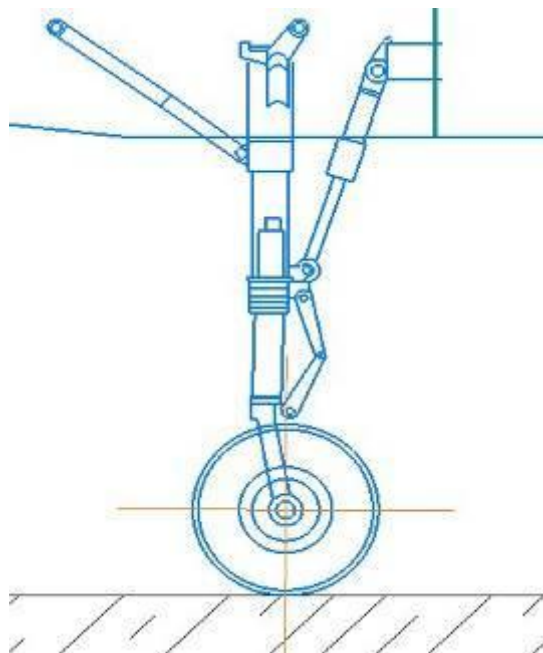


Figure 1.11 – Landing gear

Conclusion: My new aircraft named the “MK10-200” is a commercial mid-range passenger aircraft with a maximum capacity of 160 passengers. Fully equipped with two CFM 56-7B18 engines (86 kN thrust), the aircraft attains a range of 5600 km, cruise speed of 830 km/hr, cruise altitude of 11.9 km and a take-off distance of 1.95 km.

The calculated parameters of my aircraft in zero and first approximation are as follows; take-off mass m_0 – 739600 kg, mass of payload m_C - 25000 kg, mass of crew members m_{CR} – 400 kg, mass of aircraft's structure m_{airf} – 49152 kg, mass of fuel m_f – 106496 kg, mass of power plant m_{pp} – 10240 kg, and finally, mass of equipment m_{eq} – 18432 kg.

I was able to determine all my parameters using prototypes of medium-range passenger aircrafts of very similar characteristics in order to achieve my desired goal.

2. RESEARCH SECTION

2.1. General information about the wing lift system

2.1.1. Introduction of aircraft wing lift system

With the concept of green aviation, green aviation technology was born. Green aviation mainly refers to the general term for various professional technologies adopted by civil aircraft in the development, operation and maintenance of civil aircraft to achieve the purpose of energy saving, emission reduction and noise reduction. Green aviation technology involves all aspects of the aviation field and is the foundation and prerequisite for realizing green aviation, mainly including green pneumatic technology, green multi-electric technology, green manufacturing technology and green maintenance technology. Europe and the United States and other countries actively respond to the green environmental protection goals of world aviation, focusing on relevant technical research in the direction of new aircraft layout, power system, raw material selection, new technology application and noise reduction.

With the advent of the era of multi-electric and all-electric aircraft, the aircraft electromechanical system is moving towards multi-electric/all-electric, intelligent and integrated development, the purpose of which is to obtain the optimal performance of the aircraft through the comprehensive optimization of the four aspects of function, energy,

control and physics, and promote it into a green aircraft electromechanical system. The current trend of green aviation has involved electromechanical systems and avionics systems[1].

The high lift system is one of the key flight control systems that affect the flight safety of the aircraft and belongs to the typical electromechanical hydraulic system. By controlling the deflection of the flap wing, the wing curvature is changed and the wing area is increased, so as to realize the lift increase in the take-off phase, the lift increase and drag reduction in the landing stage. When traditional R&D personnel mention green aviation, it is generally understood as drag reduction, fuel consumption reduction, pollution reduction and noise reduction. On the one hand, the advanced refined lifting device can realize the coordinated optimization of take-off and landing and cruise performance, improve low-speed take-off and landing performance, improve cruise efficiency and reduce fuel consumption; On the other hand, the wing segment is reduced, and the airfoil drive and motion mechanism are simplified, thereby reducing weight, increasing effective load, and reducing maintenance costs. Moreover, the leading edge slits and trailing edge flaps of the existing aircraft are the main noise sources of civil aircraft, and the advanced and refined lifting device is one of the key factors of aircraft noise reduction, and the optimal aircraft performance can be obtained through comprehensive optimization of functions, energy,

control and physics. Therefore, the high-lift system has an important impact on the realization of green aviation technologies such as aerodynamic characteristics, flight quality, safety, energy saving and noise of civil aircraft[3].

2.1.2. Research Inadequacies

Single, double and triple slit flaps are limited by air surface gaps, movement structures and space on board, which are difficult to meet the needs of new generation or future aircraft such as efficient ascension and noise reduction; Once the mechanical transmission system is stuck or broken, the flap wing will lose the function of retracting, and the airfoil surface reconstruction cannot be realized, which reduces the survivability and safety of the aircraft. Most of the control systems of the aircraft are controlled by independent computers, which is not easy to realize the interactive and shared control of the aircraft's multi-airfoil, improve the reconstruction of the airfoil, and improve the survivability and safety of the aircraft. The application degree of intelligent technology is not high, can not achieve online monitoring and prediction of faults, especially some hidden faults, only when the fault occurs, can be found, seriously affecting the aircraft dispatch rate and flight line security; The application of advanced material technology is insufficient, resulting in heavy aircraft weight, increased fuel, poor economy and environmental protection, and

it is necessary to further improve the application of advanced composite materials. Based on the technical limitations and constraints of the existing high-lift system, it is difficult to meet the requirements of efficient increase, energy saving and noise reduction of green aviation, so it is urgent to carry out new technology research[1].

2.2. Concept Design of Adaptive Wing with Flexible Trailing Edge

2.2.1. Introduction of Adaptive Wing with Flexible Trailing Edge

Relevant research and flight verification tests show that adaptive wings can significantly enhance flight control capabilities; In all flight packages, Reduction of aerodynamic resistance within the line range; Reduced structural weight; means of broadening the wing design when the extension and sweep angle are fixed; Inhibit flutter and increase flutter critical velocity; Slow down wind surge loads and maneuvering loads and improve aircraft maneuverability, so I will apply intelligent flexible adaptive wings to the aircraft I design[4].

2.2.2. Drop-down hinge flap and spoiler offset configuration

The A350 XWB aircraft flap drive mechanism uses an adaptive lower Sunken hinged flaps (see Figure 2.1) that allow the flap kinematic mechanism[5]. Less complexity and less weight sunken hinged flap facing One challenge is to control the gap between the spoiler trailing

edge and the flap. If the gap is too large, it will cause turbulence in the airflow of the flap attachment layer, flow, reducing the lift-to-drag ratio of the aircraft. The A350XWB adopts the spoiler down bias technology, through the spoiler Drooping, on the one hand increases the camber of the wing and on the other hand reduces the turbulence. The gap between the trailing edge of the plate and the flaps for an optimized aircraft wing surface. Laminar flow increases the lift-to-drag ratio[6].

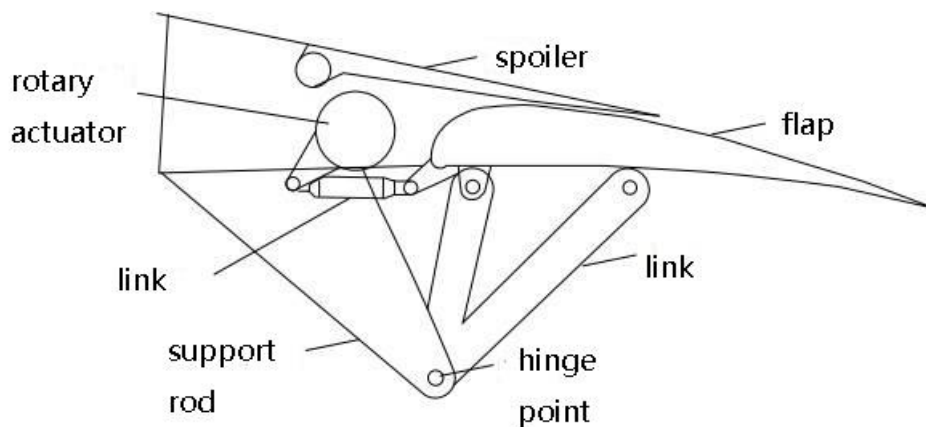


Figure 2.1 - A350XWB Drop-down hinge flap and spoiler offset configuration

2.2.3. *Trailing edge flap variable camber technology*

In the cruising stage, when the cruising speed is constant, with the the fuel consumption of the machine is reduced, the weight is reduced, and the traditional fixed-wing type[7]. For aircraft, the lift coefficient often does not change much in order to reduce fuel consumption. Generally, by increasing the cruising altitude and reducing the flight resistance, improve economy, but this method does not reduce the

aerodynamic load of the aircraft. Distribution, lift-drag efficiency, and fuel consumption are optimized[8]. The A350XWB aircraft adopts the trailing edge flap variable camber technology, through Differential inner and outer flaps (see Figure 2.2) for improved cruise phase. The shape of the lift distribution reduces the wing root bending moment and reduces the wing stress. reduces fatigue, reduces the weight of the wing structure, and also utilizes the flap differential. The control technology realizes the function of roll auxiliary trimming. when the plane leaves Lateral fuel imbalance, single engine failure, or single aileron activation When the connecting rod breaks, the motor controller is used to control the motor. Drive the active differential gearbox to realize the up and down deflection of the outer flaps, The auxiliary left and right ailerons realize the function of trimming the aircraft, realizing the The overall gain of the aircraft is about 10% under standard flight conditions and cruising conditions The overall income of getting off the plane is 1% to 3% [9].

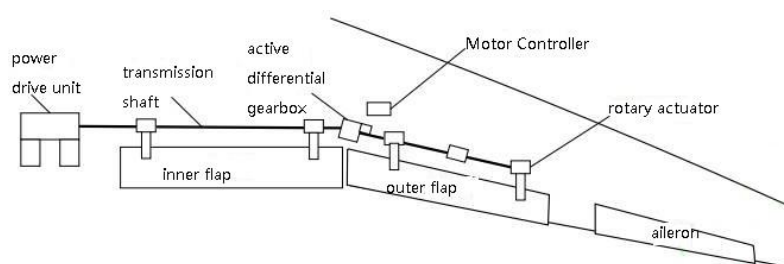


Figure 2.2 - A350XWB flap system configuration

2.2.4. Intelligent flexible adaptive wing

Coordinated deformation problem between mid-wing skin and support-driven structure. S. Kota [10]. With the support of the US Air Force Laboratory Fund, Based on NACA63418 using a flexible mechanism, a bendable front edge flexible structure, wind tunnel experiments show that the use of flexible wing technology. The technique can improve the lift-to-drag ratio by about 51% and the lift coefficient by about 25%. H. P. Monner [11] proposed the concept of "finger" wing deformation (see Figure 2.3 for details), this kind of flexible wing structure can realize the chord direction deformation can also be differentially deformed along the span direction, finally realizing the machine adaptive deformation torsion of the wing. Huang Jian proposed a new type of zero berth Song ratio honeycomb structure variable camber wing structure solves the problem of variable camber machine. Coordinated deformation problem between mid-wing skin and support-driven structure [12].

Conventional flaps of traditional aircraft are generally developed by serial models. A specific model optimized for the extended version, for a small number of passengers, needed to use a specific machine with a larger size and heavier weight. type modification, the result is an increase in the weight of the passenger seat, an increase in fuel consumption, which will increase to some extent due to the higher take-off weight, Landing costs and aircraft with adaptive wings will be more

expensive than conventional. The standard wing is easier to achieve under different stages of the aircraft and under different load conditions. The adaptive deformation of the wings is more flexible and more suitable for the needs of subsequent aircraft modifications. Since 1985, European and American countries have developed intelligent wing structures (ADIF), smart leading edge device (Smart LED), smart highLift Device (SADE) and Smart Deformation and Sensing Technology (SMS). Research on the direction of intelligent wings; German Aerospace Research Institute Developed Smart Leading Edge (SmartLED) for future transport class aircraft research, achieved the deformation requirement of 20° down; Germany (Fraunhofer) Research Institute relies on the EU Clean Sky Program to develop. Carried out research on the continuous variable camber technology of regional aircraft wings and completed Ground demonstration verified [13]; EU targets next-generation civil aircraft with high lift. System proposes the smart drooping wing concept in seven framework plans. The idea is to realize the seamless and flexible deformation of the leading edge high-lift device, Reduce flight resistance and reduce noise. With the development of smart materials, driving structures, and control technologies [14], Europe has carried out research on the design and manufacture of flexible trailing-edge deformable wings. study. Generally through functional materials, new structures, mechanical machines. Structural deformation optimization, flexible

materials and advanced high-efficiency drive devices, After a comprehensive balance of advanced sensors and flight controls, the Positive gains from adaptive wings The high lift system is used. It is a system for realizing the control, drive, and actuation of airfoil movements, and With the intelligent flexible adaptive wing technology proposed, it will be Change the control, drive, and actuation methods of traditional high-lift systems, New technologies are also proposed for the next generation or future aircraft high-lift system. challenge [15,16].

For this reason, the next generation or future aircraft may gradually In the sense of the development of intelligent flexible wings with fully enclosed configuration, from so that the aircraft can obtain the best aerodynamic airfoil at different flight stages, and Positive benefits such as noise reduction [17].

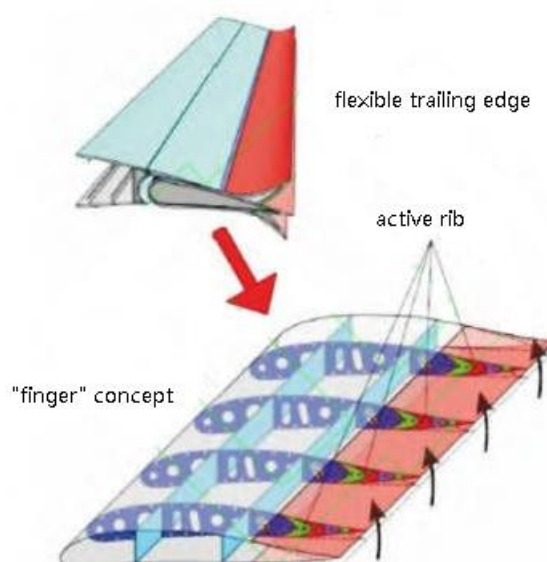


Figure 2.3 - The concept of "finger" variable camber

2.2.5. Flexible ribbed adaptive wing concept

Figure 2.4 shows an adaptive wing with a flexible rib trailing edge that allows the wing curvature to vary not only along chords, but also differential along spread direction to achieve adaptive torsion of the wing turn, and ensure that the wing has a smooth airfoil profile without adding additional gaps, and if the technical research is mature, it can be used to replace the traditional flap and aileron control surfaces. The skin of the trailing edge of the wing is supported by these actively deformed flexible ribs, which are made up of a number of independent rigid units connected to each other by hinges and sliding hinges, and each rib can be driven individually. The flexible wing rib relies on the deflection movement of its internal units and achieves the expected shape change in wing profile with certain kinematic laws. In Figure 2.4, the third element is used as an example to illustrate the principle of the composition of the flexible wing rib unit. The wing rib unit consists of an "inner plate" and two "outer plates", each with four connecting holes, two of which are used to mount the sliding hinge and two on the inside for the hinge.

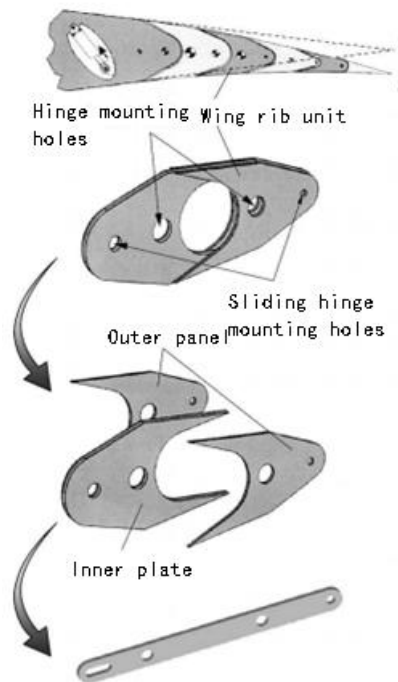


Figure 2.4 - Rotatable rib structure

2.2.6. Kinematic study of rotatable wing rib mechanism

The rotatable wing rib consists of multiple subunits, each consisting of a combination of 2 outer plates and 1 inner plate, as shown in Figure 1. Each rib unit is a rod with a local airfoil profile with 2 shaft mounting holes and 2 sliding hinge mounting holes. The evolution mechanism of each 3 adjacent elements forming a planar connecting rod slider through the rotating shaft and sliding hinge is shown in Figure 2. Use numbers for ease of illustration and letters to the unit and motion subnumber. A is the connection point between the rib and the fixed spar of the front section, B is the driving point of the rib deflection, and the driving amount is expressed by the angular displacement $\angle BCA$. Use the hinges D, G and

I, and the vertical displacement of the trailing edge point J to describe the deflection of the wing ribs. The rotatable rib mechanism is a single-degree-of-freedom system, that is, the driving displacement at point B corresponds one-to-one to the deflection shape of the rib. Therefore, deriving the correspondence between the driving displacement amount and the deflection shape is the key to the design and motion control of the rotatable rib mechanism.

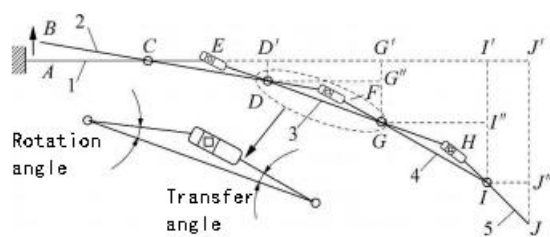


Figure 2.5 – Kinematic model of rotating rib

In Figure 2.5, the wing ribs are deflected after the first axis C near the leading edge, and the second axis D is the connection between element 2 and element 3. The contact has a deflection distance of DD' . The deflection distance of the third shaft G connecting unit 3 and unit 4 is

$$GG' = GG'' + G''G' = GG'' + DD' \quad (2.1)$$

As can be seen from Equation (2.1), the deflection distance of the axis G is equal to the sum of the deflection distance DD' of the axis D and the self-deflection distance GG'' of the axis G relative to the horizontal position. By analogy, the deflection distance of the 4th, 5th and nth axis can be expressed in this recursive relationship, i.e.

$$\text{dis}_k = \text{dis}_{k-1} + r \text{dis}_k \quad (k = 2, 3, \dots, n) \quad (2.2)$$

Where: dis_k is the deflection distance of the k th axis relative to the initial position; $R \text{dis}_k$ is the self-deflection distance of the k th axis relative to the horizontal position (hereinafter referred to as the rotation distance).

The deflection distance of point A solid support of element 1 at the fixed segment axis C is equal to zero, that is, when $k = 1$, $\text{dis}_1 = 0$. Thus the deflection distance of the axis D is the self-distance and its geometric relation is

$$DD' = CD \times \sin \angle ECD = CD \times \sin \angle BCA \quad (2.3)$$

Similarly, the rotation distance and rotation angle of the axis G are respectively

$$GG'' = DG \times \sin \angle G''DG \quad (2.4)$$

$$\angle G''DG = \angle G''DF + \angle FDG = \angle EDC + \angle ECD \quad (2.5)$$

$\angle EDC$ in equation (2.5) is called the transfer angle. Its recursive relationship is

$$r \text{dis}_k = l_{ksi} \sin(\angle ra_{k-1} + \angle ta_{k-1}) \quad (k = 2, 3, \dots, n) \quad (2.6)$$

Where l_k is the distance between the k th and $k+1$ spindles; $\angle ra_{k-1}$ is the rotation angle of the $k-1$ axis; $\angle ta_{k-1}$ is the transfer angle of the $k-1$ axis.

Based on the above derivation, the following two conclusions are drawn:

- a) As can be seen from Figure 2.5, $\angle rak-1$ and $\angle tak-1$ in equation (2.6) are determined by the spacing lk of the hinge points and the spacing of the hinge points and hinge points, so different wing rib deformation shapes can be achieved by changing the spacing layout of the rib element constraint points.
- b) The more subunits that make up the rotatable ribs, the larger n and the smaller the shaft spacing lk , the smoother the deflected trailing edge airfoil profile. In addition, calculating the deflection deflection form of the wing rib according to the recursive function expressions (2.2) and equation (2.6) of the motion relationship between wing rib elements is a process that is passed sequentially from front to back. But in practice, the constraint relationship between the elements determines that the mechanism is a single-degree-of-freedom system, so the motion of the individual elements is synchronized.

2.3. Design of wing geometric parameters

The wing surface area of the projected plane is;

$$S = m_0 * g / (10 p_0) \quad (2.7)$$

$$\text{Where } g = 9.8 \text{ m/s}^2$$

$$p_0 = 1796.5 \text{ N/m}^2$$

$$S = 204800 \times 9.8 / (10 \times 1796.5)$$

$$S = 111.72 \text{ m}^2$$

The wingspan (L)

$$L = \sqrt{\lambda S} \quad (2.8)$$

Where the value of λ is taken from table (1.3), $\lambda = 9.45$

$$L = \sqrt{(9.45 * 111.72)} = 32.492 \text{ m.}$$

Root (on axis of airplane symmetry) b_0 and tip b_k wing chords are determined using the values S , η , L ;

$$b_0 = \frac{S}{L} * \frac{2\eta}{\eta+1} \quad (2.9)$$

$$b_0 = (111.72 / 32.492) * (2 \times 6.3 / 6.3 + 1) = 5.93 \text{ m}$$

$$b_k = \frac{b_0}{\eta} \quad (2.10)$$

$$b_k = 5.93 / 6.3 = 0.94 \text{ m}$$

Where value $\eta = 6.3$ taken from table (1.3)

Wing mean aerodynamic chord (MAC) is calculated by the formula

$$b_A = \frac{2}{3} * b_0 \frac{\eta^2 + \eta + 1}{\eta(\eta + 1)} \quad (2.11)$$

$$b_A = (2/3) \times 5.93 \times ((6.3^2 + 6.3 + 1) / 6.3 * (6.3 + 1))$$

$$b_A = 4.04 \text{ m}$$

Coordinate of MAC along a wing span is determined by the relation

$$Z_A = \frac{L}{6} * \frac{\eta+2}{\eta+1} \quad (2.12)$$

$$Z_A = (32.492 / 6) * (6.3+2 / 6.3+1)$$

$$Z_A = 6.16 \text{ m}$$

Coordinate of MAC nose along an axis 0_x

$$X_A = Z_A * \tan \chi_{LE} \quad (2.13)$$

$$X_A = 6.16 * \tan (32.07)$$

$$X_A = 3.86 \text{ m}$$

Where χ_{LE} (sweep angle of the wing's leading edge = 32.07°)

$$\chi_{LE} = \tan^{-1} (\tan \chi + (\eta - 1) / \lambda(\eta + 1)) \quad (2.14)$$

$$\chi_{LE} = \tan^{-1} (\tan (25.020) + (6.3 - 1) / 9.45 * (6.3 + 1)) = 32.07^\circ$$

(Where χ is the sweep angle of the wing's quarter-chord line and is taken from Table 1.3 $\chi = 25.02^\circ$).

The 3D view of the resulting wing and aircraft is shown in the figure 2.6.

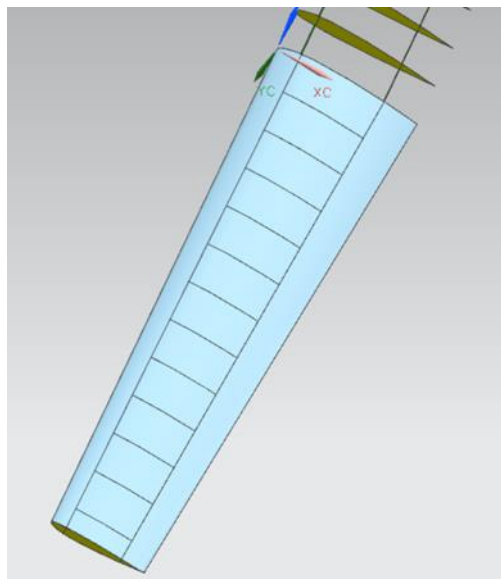


Figure 2.6 (a) - the 3D view of the wing

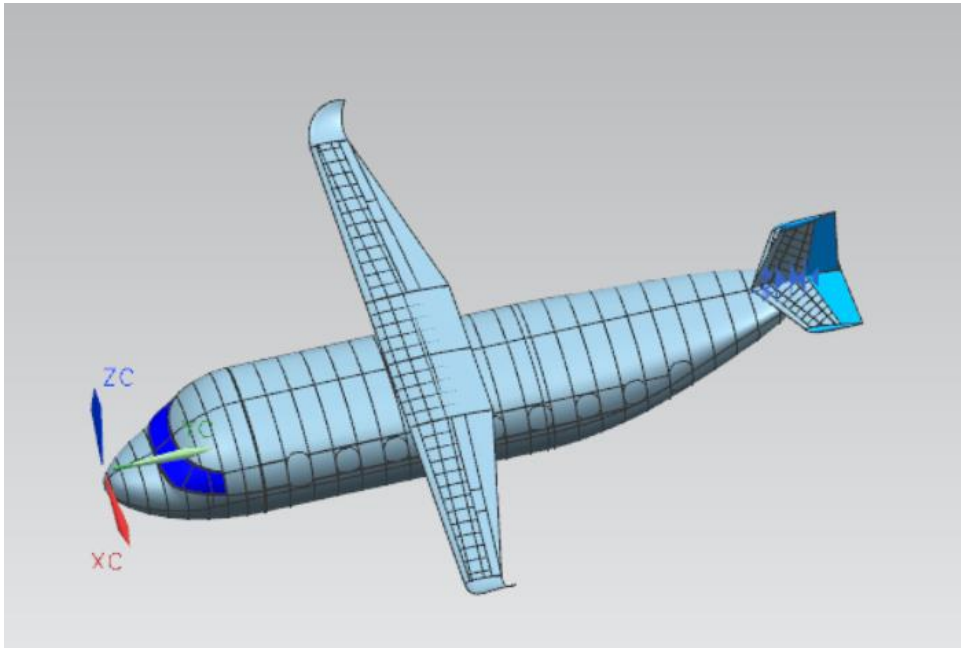


Figure 2.6 (b) - the 3D view of the aircraft

2.4. Wing and high-lift devices parameters influence on C_y

In this lab work I am analysing the take-off characteristic of my plane with respect to the wing geometrical parameters. The main parameter for analysis which I have considered is Relative Thickness of Chord.

Relative thickness of Chord or better known as Airfoil thickness ratio is given by, $C = \text{Maximum Thickness} / \text{Chord}$.

Airfoil thickness ratio has a direct effect on drag, maximum lift, stall characteristics and structural weight. The drag increases with increasing thickness due to increased separation. The thickness ratio has a great effect on the Critical Mach Number (mac number at which supersonic flow first appears over the wing.)

The thickness ratio affects the maximum lift and stall characteristics primarily by its effect on the nose shape. For a wing of fairly high aspect ratio and moderate sweep, a larger nose radius provides a higher stall angle and a greater maximum lift coefficient.

2.The second Characteristic that we are analysing for the required aircraft is the Wing loading.

Wing loading is the weight of the aircraft divided by the area of the reference (not exposed) wing. Wing loading affects stall speed, climb rate, take-off and landing distances, and turn performance. The wing loading

determines the design lift coefficient, and impacts drag through its effect upon wing span.

Wing loading has a great effect on the Total Take off Mass of the Aircraft. If the wing loading is reduced, the wing is larger. This may improve performance but the additional drag and empty weight due to the larger wing will increase take off gross weight. To ensure that the wing provides enough lift in all circumstances, the designer should select the lowest of the estimated wing loadings.

To maximise range during cruise the wing loading should be selected to provide a high L/D at the cruise conditions.

3. The next important parameter that we analyse in this lab is the lift to drag ratio

In aerodynamics, the lift-to-drag ratio, or L/D ratio, is the amount of lift generated by a wing or vehicle, divided by the drag it creates by moving through the air. A higher or more favourable L/D ratio is typically one of the major goals in aircraft design; since a particular aircraft's required lift is set by its weight, delivering that lift with lower drag leads directly to better fuel economy, climb performance, and glide ratio.

4. The last parameter that we are analysing is the Coefficient of lift.

The lift coefficient is a dimensionless coefficient that relates the lift generated by a lifting body to the density of the fluid around the body, its velocity and an associated reference area.

INPUT: see in the figure 2.7.

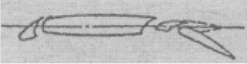
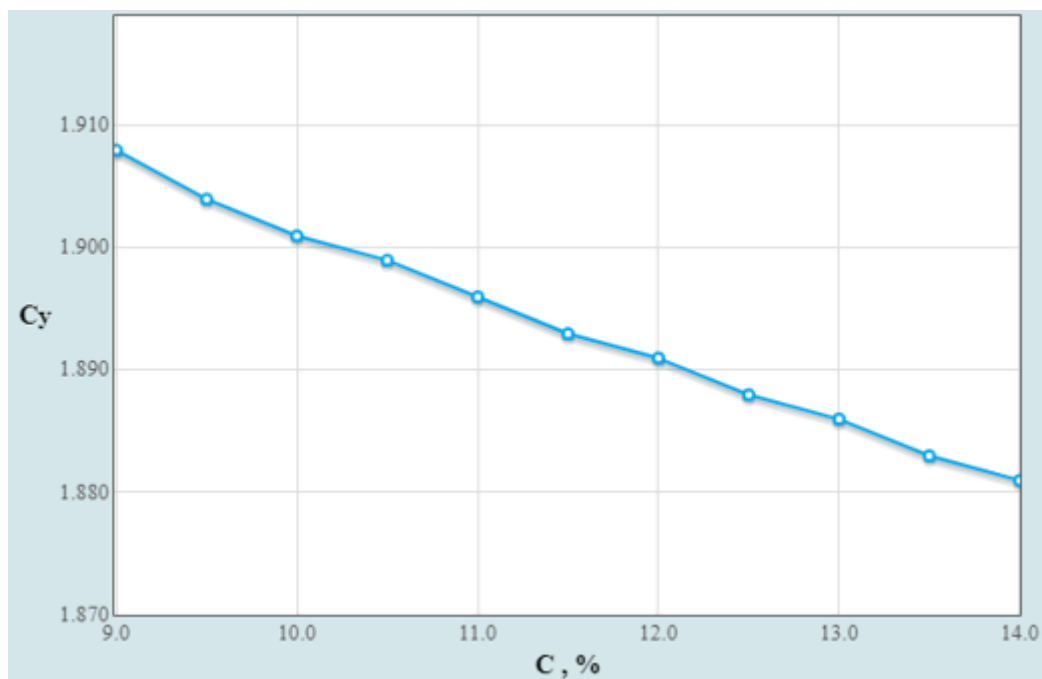
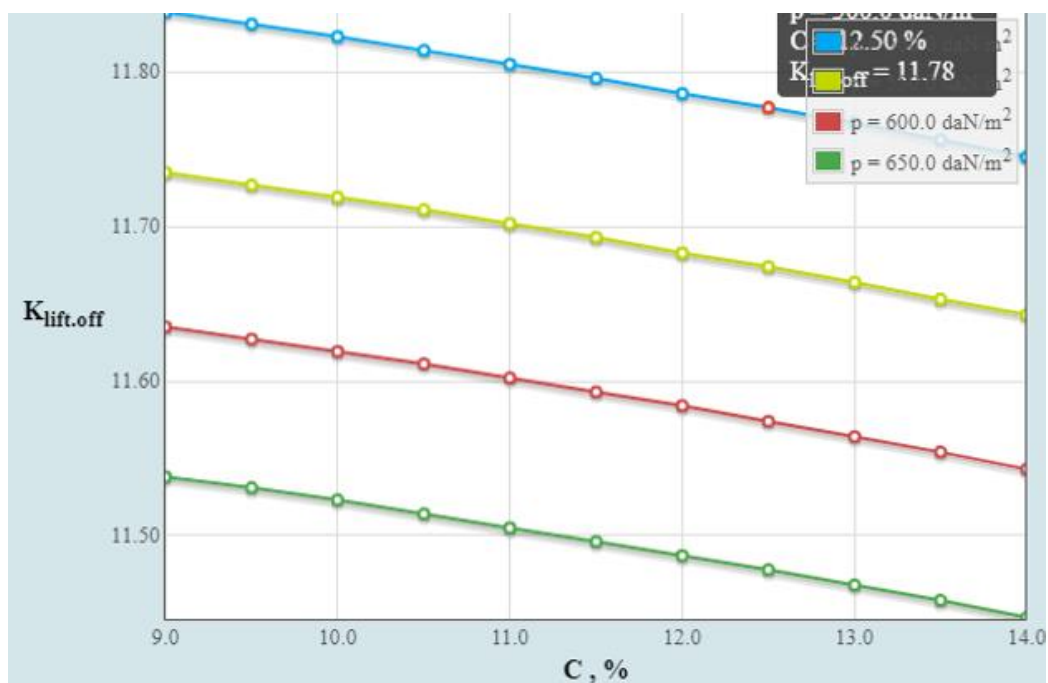
Airplane category selecting and it's parameters editing:			
Select airplane type:		Passenger	▼
$n_{\text{pass. (itm.)}}$:	[?] 200	$m_{\text{pass. (kg)}}$:	[?] 120
Wing high-lift devices parameters:			
Choose wing high-lift devices type:		Slat and double slotted retractable flap	▼
			
$\Delta \bar{C}_y 1.\text{dev.}$:	[?] 2	$dC_y = 1.800 \dots 2.200$	
$\bar{l}_{\text{sl.}}$:	[?] 0.7	$k_{\text{sl.}}$:	[?] 0.15
$b_{\text{fl.}}$:	[?] 0.24	$b_{\text{fl. tab.}}$:	[?] 0.300
$\delta_{\text{fl. TO (deg.)}}$:	[?] 25	$\delta_{\text{fl. TO, tabl. (deg.)}}$:	[?] 40.00
$\bar{l}_{\text{fl.}}$:	[?] 0.7	$k_{\text{fl.}}$:	[?] 0.15
Initial data:			
\bar{C} (%):	[?] 12.5	λ_w :	[?] 9.45
η :	[?] 6.3	$\chi_{\text{je (deg.)}}$:	[?] 25
$\alpha_{\text{TO (deg.)}}$:	[?] 9	M_{TO} :	[?] 0.2
$d_{\text{fus. (m)}}$:	[?] 4	$\lambda_{\text{fus.}}$:	[?] 10.2
$k_{\text{mid. (daN/m}^2\text{)}}$:	[?] 5000	$k_{\text{int.w.}}$:	[?] 0.65
$k_{\text{stab.}}$:	[?] 1.35	$k_{\text{pl.}}$:	[?] 0.15
h :	[?] 5	l :	[?] 7
$\bar{l}_{\text{slots.}}$:	[?] 0.75		
Engine type selecting and dependant parameters editing:			
Choose engine type:		Turbo-fan/jet	▼
Iterative computations parameters:			
Parameter being studied:		C - Airfoil relative thickness	▼
Initial value:	[?] 9	Final value:	[?] 14
Increment:	[?] 0.5	Initial p:	[?] 100
Final p:	[?] 800	Increment p:	[?] 50

Figure 2.7 - Initial data related to wing parameters

RESULT: see in the figure 2.8.

Figure 2.8 - Diagram of C_y and C Figure 2.8 – Diagram of $K_{lift.off}$ and C

CONCLUSION: Considering the above graphs drawn from the results obtained from the software we get C_y ranging from 1.870 to 1.910 for relative thickness of chord ranging from 9 to 14. From the general view of the aircraft, we get the relative thickness as 12.5% for which the value of C_y should be around 1.889. The second graph gives us result between the wing loading and lift to drag ratio. We can select from the range of 600 to 700. The lift to drag ratio comes around 10 to 11.5. It said that the aircraft has a large lift, but the value is a little large, which may have an impact on the aircraft structure, and the lift-drag ratio needs to be determined in coordination with the aircraft structure.

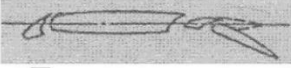
2.5. Wing and high-lift devices parameters influence on required starting thrust.

The thrust-to-weight ratio and wing loading are the two most important parameters in determining the performance of an aircraft. For example, the thrust-to-weight ratio of a combat aircraft is a good indicator of the manoeuvrability of the aircraft. The thrust-to-weight ratio varies continually during a flight. Thrust varies with throttle setting, airspeed, altitude and air temperature. Weight varies with fuel burn and changes of payload. For aircraft, the quoted thrust-to-weight ratio is often the maximum static thrust at sea-level divided by the maximum take-off weight.

In cruising flight, the thrust-to-weight ratio of an aircraft is the inverse of the lift-to-drag ratio because thrust is equal to drag, and weight is equal to lift.

INPUT: See in the figure 2.9.

Airplane category selecting and its parameters editing:		
Select airplane type:		Passenger
$n_{\text{pass. (itm.)}}$:	[?] 200	
$m_{\text{pass. (kg)}}$:	[?] 120	

Wing high-lift devices parameters:		
Choose wing high-lift devices type:		Slat and double slotted retractable flap
		
$\Delta \bar{C}_{y \text{ l.dev.}}$:	[?] 2	$dC_y = 1.800 \dots 2.200$
$\bar{l}_{\text{sl.}}$:	[?] 0.7	
$k_{\text{sl.}}$:	[?] 0.15	
$\bar{b}_{\text{fl.}}$:	[?] 0.24	
$\bar{b}_{\text{fl., tab.}}$:	[?] 0.300	
$\delta_{\text{fl. TO (deg.)}}$:	[?] 25	
$\delta_{\text{fl. TO, tabl. (deg.)}}$:	[?] 40.00	
$\bar{l}_{\text{fl.}}$:	[?] 0.7	
$k_{\text{fl.}}$:	[?] 0.15	

Initial data:		
\bar{C} (%):	[?] 12.5	
λ_w :	[?] 9.45	
η :	[?] 6.3	
$\chi_{\text{le (deg.)}}$:	[?] 25	
$\alpha_{\text{TO (deg.)}}$:	[?] 9	
M_{TO} :	[?] 0.2	
$d_{\text{fus. (m)}}$:	[?] 4	
$\lambda_{\text{fus.}}$:	[?] 10.2	
$k_{\text{mid. (daN/m}^2\text{)}}$:	[?] 5000	

Figure 2.9(a) - Initial data related to engine parameters

$k_{int.w}$:	[?]	<input type="text" value="0.65"/>
k_{stab} :	[?]	<input type="text" value="1.35"/>
k_{pl} :	[?]	<input type="text" value="0.15"/>
\bar{h} :	[?]	<input type="text" value="0.75"/>
\bar{l} :	[?]	<input type="text" value="7"/>
\bar{l}_{slots} :	[?]	<input type="text" value="0.75"/>
λ_n :	[?]	<input type="text" value="1.5"/>
L_{TO} (m):	[?]	<input type="text" value="2450"/>
f_{tr} :	[?]	<input type="text" value="0.02"/>
$\tan(\Theta)$:	[?]	<input type="text" value="0.024"/>

Engine type selecting and dependant parameters editing:

Choose engine type:		<input type="button" value="Turbo-fan/jet"/> ▼
$n_{eng.}$ (itm.):	[?]	<input type="text" value="2"/>
ξ_{int} :	[?]	<input type="text" value="0.98"/>
$\xi_{tr.cr}$:	[?]	<input type="text" value="0.7"/>
$\xi_{tr.TO}$:	[?]	<input type="text" value="0.98"/>
y :	[?]	<input type="text" value="9"/>
M_{cr} :	[?]	<input type="text" value="0.84"/>
H_{init} (km):	[?]	<input type="text" value="12"/>
H_{fin} (km):	[?]	<input type="text" value="12"/>

Iterative computations parameters:

Parameter being studied:		<input type="button" value="C - Airfoil relative thickness"/> ▼
Initial value:	[?]	<input type="text" value="9"/>
Final value:	[?]	<input type="text" value="14"/>
Increment:	[?]	<input type="text" value="0.5"/>
Initial p :	[?]	<input type="text" value="100"/>
Final p :	[?]	<input type="text" value="800"/>
Increment p :	[?]	<input type="text" value="50"/>

Figure 2.9(b) - Initial data related to engine parameters

RESULT: See in the figure 2.10.

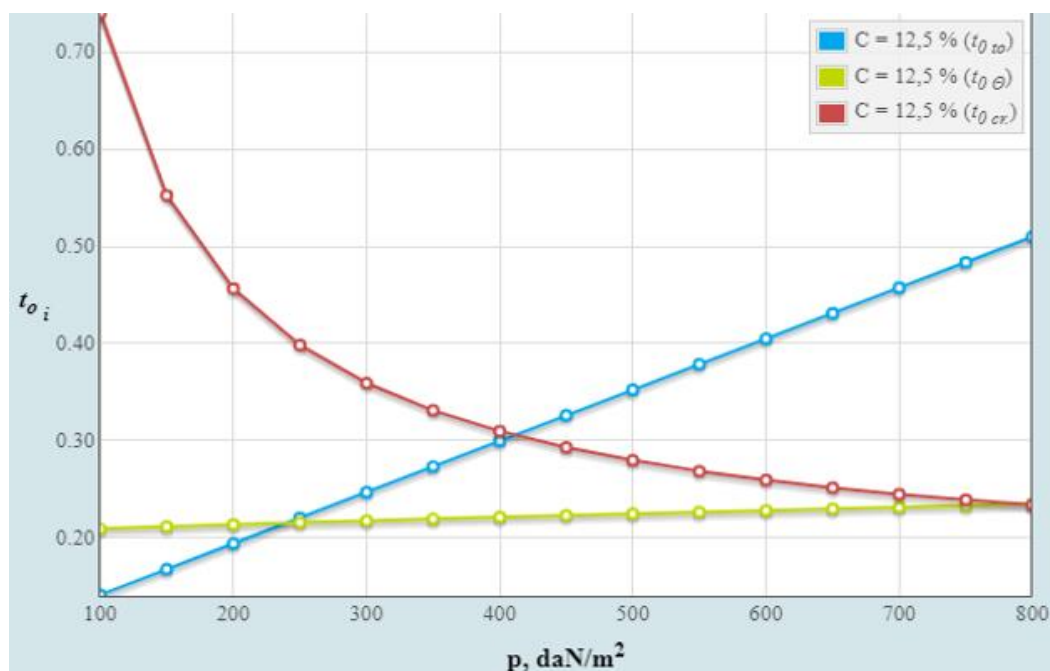


Figure 2.10 – Diagram of the thrust to weight ratio and wing loading

CONCLUSION: Above we have obtained results for the thrust to weight ratio with the wing loading. From the graphs considering the relative thickness of the chord as 12.5%. we see that the thrust to weight ratio should be around 0.2 to 0.5 for a wing loading of 700. When we compare to the prototypes, it has a reasonable range.

2.6. Airplane parameters influence on power unit relative mass.

To design the power plant, the following input basic initial data are required the purpose of the aircraft flight characteristics and aircraft take-off weight, the requirements for power plant design are shown in figure 2.11.

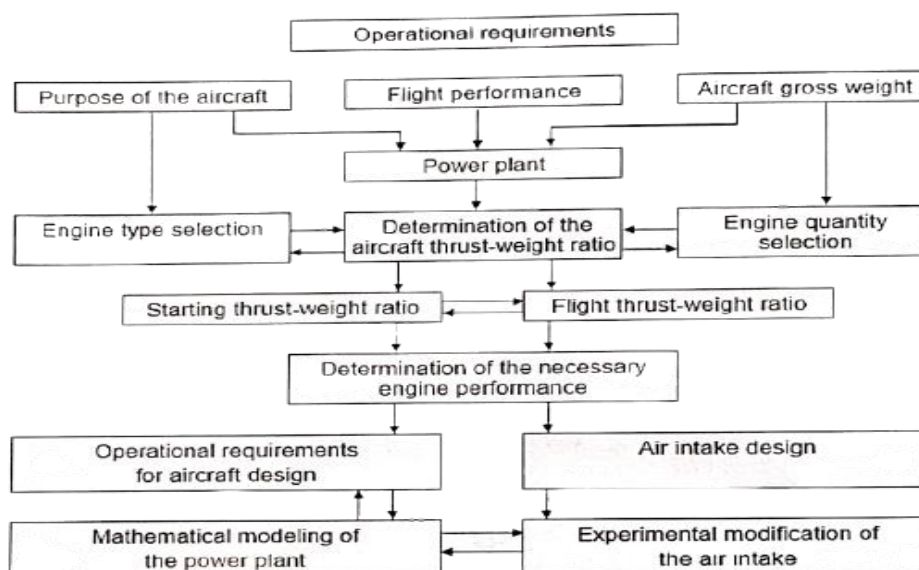


Figure 2.11 – Scheme of the engine design requirements

INPUT: See in the figure 2.12.

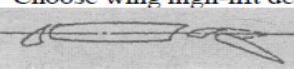
Airplane category selecting and it's parameters editing:		
Select airplane type:		Passenger
$n_{pass. (itm.)}$:	[?] 200	
$m_{pass. (kg)}$:	[?] 120	
Wing high-lift devices parameters:		
Choose wing high-lift devices type:		Slat and double sloted retractable flap
		
$\Delta \bar{C}_y 1.dev.$:	[?] 2	$dC_y = 1.800 \dots 2.200$
$\bar{l}_{sl.}$:	[?] 0.7	
$k_{sl.}$:	[?] 0.15	
$\bar{b}_{fl.}$:	[?] 0.24	
$\bar{b}_{fl, tab.}$:	[?] 0.300	
$\delta_{fl, TO} (deg.)$:	[?] 25	
$\delta_{fl, TO, tabl.} (deg.)$:	[?] 40.00	
$\bar{l}_{fl.}$:	[?] 0.7	
$k_{fl.}$:	[?] 0.15	
Initial data:		
$\bar{C} (\%)$:	[?] 12.5	
λ_w :	[?] 9.45	
η :	[?] 6.3	
$\chi_{le} (deg.)$:	[?] 25	
$\alpha_{TO} (deg.)$:	[?] 9	
M_{TO} :	[?] 0.2	
$d_{fus. (m)}$:	[?] 4	
$\lambda_{fus.}$:	[?] 10.2	
$k_{mid. (daN/m^2)}$:	[?] 5000	
$k_{int.w.}$:	[?] 0.65	

Figure 2.12(a) – Initial data related to engine parameters

$k_{stab.}$:	[?] 1.35
$k_{pl.}$:	[?] 0.15
\bar{h} :	[?] 0.75
\bar{l} :	[?] 7
$\bar{l}_{slots.}$:	[?] 0.75
$\lambda_n.$:	[?] 1.5
L_{TO} (m):	[?] 2450
$f_{tr.}$:	[?] 0.02
$\tan(\Theta)$:	[?] 0.024

Engine type selecting and dependant parameters editing:

Choose engine type: Turbo-fan/jet ▼

$n_{eng.}$ (itm.):	[?] 2
$\gamma_{en.}$ (daN/kWt):	[?] 0.0203
$\xi_{int.}$:	[?] 0.98
$\xi_{tr.cr.}$:	[?] 0.7
$\xi_{tr.TO.}$:	[?] 0.98
γ :	[?] 9
$M_{cr.}$:	[?] 0.84
$H_{init.}$ (km):	[?] 12
$H_{fin.}$ (km):	[?] 12
k_1 :	[?] 0.25
$n_{rev.eng}$ (itm.):	[?] 2

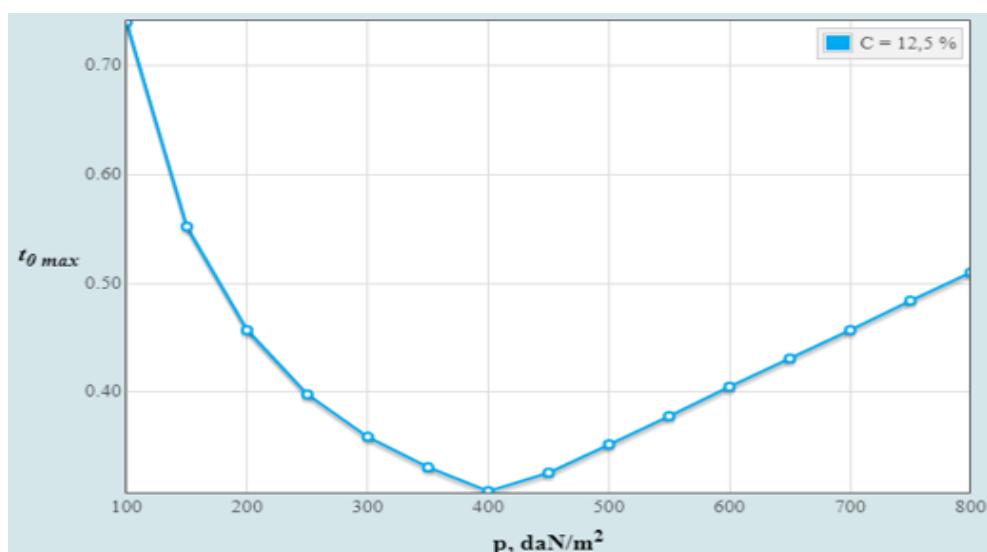
Iterative computations parameters:

Parameter being studied: C - Airfoil relative thickness ▼

Initial value:	[?] 9
Final value:	[?] 14
Increment:	[?] 0.5
Initial p:	[?] 100
Final p:	[?] 800
Increment p:	[?] 50

Figure 2.12(b) – Initial data related to engine parameters

RESULT: See in the figure 2.13.

Figure 2.13(a) – Diagram of $t_{0\max}$ and p

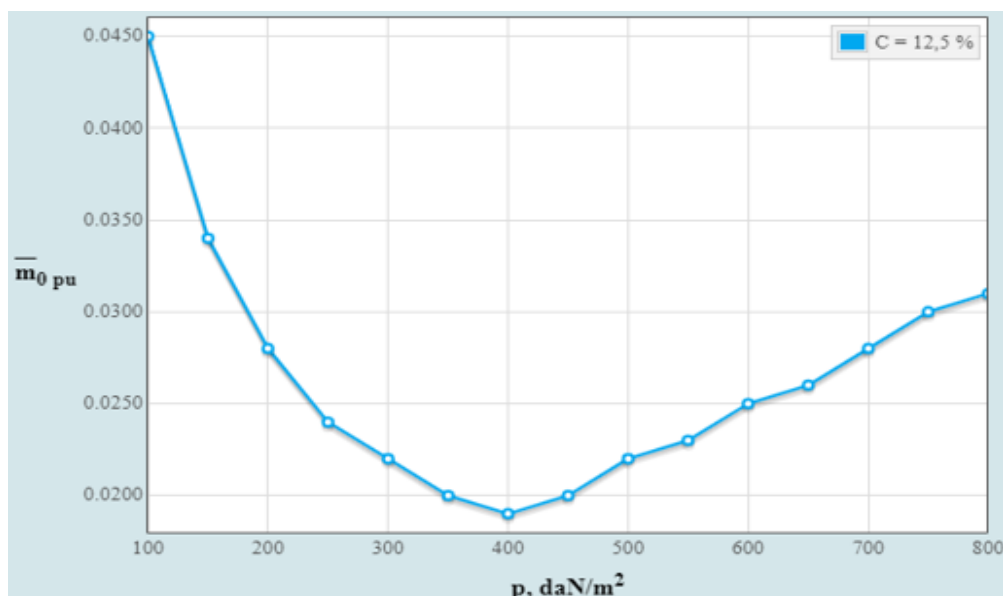


Figure 2.13(b) – Diagram of \bar{m}_{0pu} and p

CONCLUSION: We see that the maximum thrust to weight ratio should be around 0.4 to 0.5 for a wing loading of 700. From the above results we can conclude that the relative mass of power plant obtained is appropriate which is lower than zero approximation. We get the relative mass of power plant as 0.027.

2.7. Airplane parameters influence on fuel relative mass

INPUT: See in the figure 2.14.

Airplane category selecting and it's parameters editing:

Select airplane type:

$n_{pass.}$ (itm.):

$m_{pass.}$ (kg):

Initial data:

\bar{C} (%):

λ_w :

η :

$d_{fus.}$ (m):

$\lambda_{fus.}$:

$k_{mid.}$ (daN/m²):

$k_{int.w.}$:

$k_{stab.}$:

$k_{pl.}$:

$\bar{l}_{slots.}$:

λ_n :

L_c (km):

Engine type selecting and dependant parameters editing:

Choose engine type:

χ_{ie} (deg.):

γ :

$M_{cr.}$:

$H_{init.}$ (km):

$H_{fin.}$ (km):

Iterative computations parameters:

Parameter being studied:

Initial value:

Final value:

Increment:

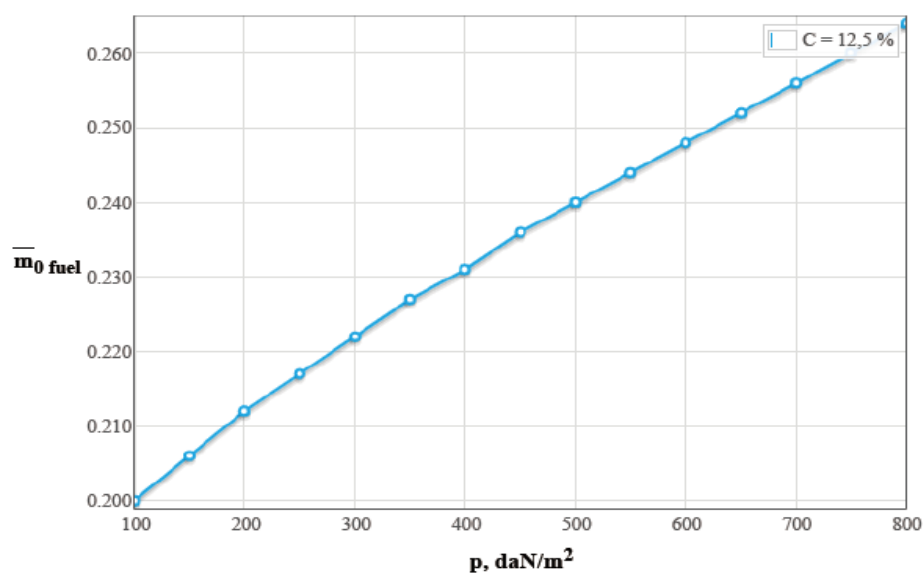
Initial p:

Final p:

Increment p:

Figure 2.14 – Initial data related to engine parameters

RESULT: See in the figure 2.15.

Figure 2.15 – Diagram of $\bar{m}_{0\text{fuel}}$ and p

CONCLUSION: From the results obtained we can conclude that the relative mass of fuel obtained is 0.255 with the wing loading 700daN/m². It is reasonable.

2.8. Airplane parameters influence on structure relative mass

$$\bar{m}_{fuel} = a + b \frac{L_{fl}}{V_{cruis}} = a + b \cdot t_{fl},$$

here $a = \begin{cases} 0.04 \dots 0.05 - \text{for light non-manuverable planes;} \\ 0.06 \dots 0.07 - \text{for any other airplane;} \end{cases}$

$b = \begin{cases} 0.05 \dots 0.06 - \text{for sub-sonic planes;} \\ 0,14 \dots 0,15 - \text{for supersonic planes;} \end{cases}$

L_{fl} – flight range in kilometers;

V_{cruis} – cruising flight speed in km/h;

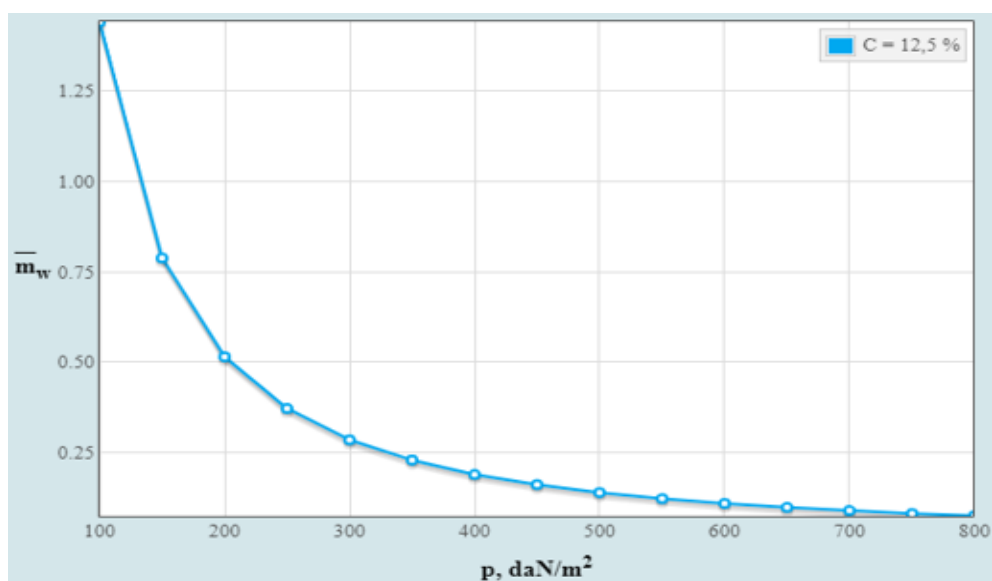
t_{fl} – planned flight duration in hours.

INPUT: See in the figure 2.16.

Airplane category selecting and it's parameters editing:			
Select airplane type:	Passenger		
$n_{pass.}$ (itm.):	[?] 200	$m_{pass.}$ (kg):	[?] 120
Initial data:			
\bar{C} (%):	[?] 12.5	λ_w :	[?] 9.45
η :	[?] 6.3	χ_{le} (deg.):	[?] 25
$d_{fus.}$ (m):	[?] 4	$\lambda_{fus.}$:	[?] 10.2
$k_{int.w.}$:	[?] 0.65	$k_{mid.}$ (daN/m ²):	[?] 5000
$k_{stab.}$:	[?] 1.35	$k_{pl.}$:	[?] 0.15
$l_{slots.}$:	[?] 0.75	λ_n :	[?] 1.5
L_c (km):	[?] 5000	C_0 (%):	[?] 12.5
$k_{fl.}$:	[?] 0.25	Choose wing panels type:	Conventional riveted panels
Choose fuel tanks type:	Torsion box integral fuel tanks with internal joints sealing		
Choose luggage accommodation type:	Luggage in containers		
Engine type selecting and dependant parameters editing:			
Choose engines configuration:	Under the wing and $d_f < 5m$		
Choose engine type:	Turbo-fan/jet		
y :	[?] 9	$M_{cr.}$:	[?] 0.84
$H_{init.}$ (km):	[?] 12	$H_{fin.}$ (km):	[?] 12
$k_{f.e.}$:	[?] 0.023		
Stabilisers parameters:			
Choose stabiliser configuration:	Low positioned stabiliser		$\bar{S}_{h.st.}$:
$\bar{S}_{v.st.}$:	[?] 0.212		[?] 0.263
Landing gear parameters:			
Main landing gear attachment place (for turboprop):	All struts attached to the wing		
Main landing gear struts attachment place:	Into the wing		
Main landing gear wheels accommodation place:	In the wing		
Main landing gear struts number:	Two main struts		
Iterative computations parameters:			
Parameter being studied:	C - Airfoil relative thickness		
Initial value:	[?] 9	Final value:	[?] 14
Increment:	[?] 0.5	Initial p:	[?] 100
Final p:	[?] 800	Increment p:	[?] 50
Initial d_f (m):	[?] 4	Final d_f (m):	[?] 7
Increment d_f (m):	[?] 0.5	Initial λ_f :	[?] 8
Final λ_f :	[?] 14	Increment λ_f :	[?] 0.5

Figure 2.16 – Initial data related to structure relative mass

RESULT: See in the figure 2.17.

Figure 2.17(a) - Diagram of \bar{m}_w and p

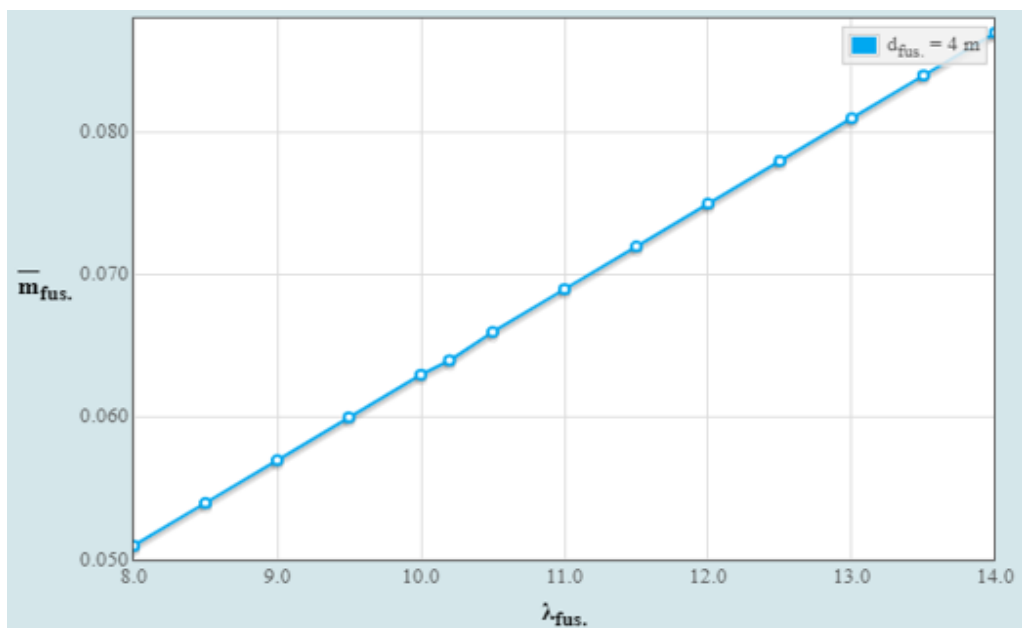


Figure 2.17(b) - Diagram of $\bar{m}_{fus.}$ and $\lambda_{fus.}$

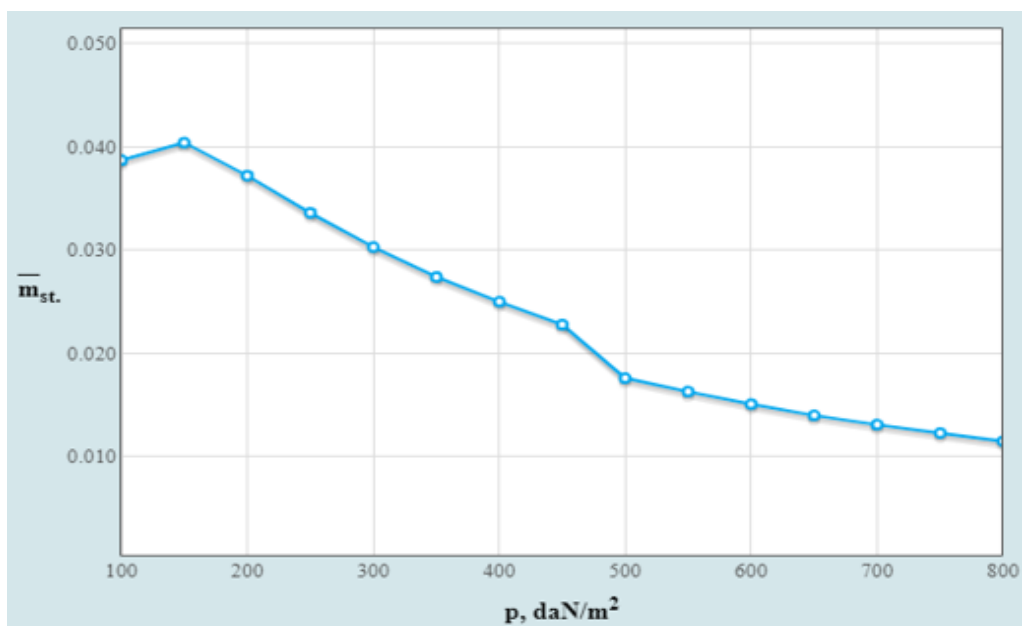


Figure 2.17(c) - Diagram of $\bar{m}_{st.}$ and p

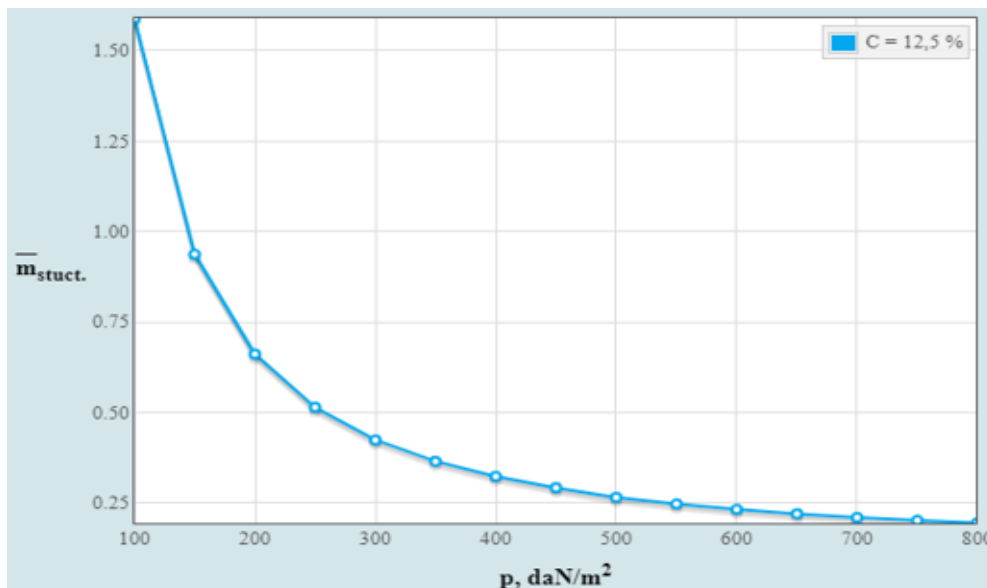


Figure 2.17(d) - Diagram of \bar{m}_{stuct} and p

CONCLUSION: From the results obtained we can conclude that the relative mass of wing obtained is less than 0.1, the relative mass of equipment obtained is around 0.015, the relative mass of payload obtained is less than 0.25 with the wing loading 700 daN/m^2 , the relative mass of fuselage obtained is around 0.065 with $\lambda_{fus}=10$. All values are within reasonable limits.

2.9. Crew, equipment and payload mass calculation.

In this lab we need to determine the mass of the equipment, control system, operational item and crew members. Mass of crew member is accepted equal to 80kg. Thus $m_{crew} = 80 \cdot n_{crew}$. The number of crew members of this aircraft is considered as 8 according to the number of passengers in the airplane.

INPUT:See in the figure 2.18.

Airplane category selecting and it's parameters editing:	
Select airplane type:	Passenger ▼
$n_{\text{pass.}}$ (itm.):	[?] 200
$m_{\text{pass.}}$ (kg):	[?] 120
Initial data:	
L_c (km):	[?] 5600
$n_{\text{cr.}}$ (itm.):	[?] 8
$k_{\text{pl.}}$:	[?] 0.15

Figure 2.18 - Initial data related to payload mass

RESULT:See in the figure 2.19.

Initial data:
Airplane type = Passenger $n_{\text{pass.}} = 200(\text{itm.}); m_{\text{pass.}} = 120(\text{kg});$
$L_c = 5600(\text{km}); n_{\text{cr.}} = 8(\text{itm.}); k_{\text{pl.}} = 0.15;$
Calculation results:
$m_{\text{cr.}} = 640(\text{kg}); m_{\text{eq.}} = 18525(\text{kg});$ Total mass of airplane load - $m_{\text{c.e.p}} = 43165(\text{kg})$

Figure 2.19 - Crew, equipment and payload mass calculations

CONCLUSION: According to prototypes, all values are reasonable.

2.10. Airplane parameters influence on take-off mass

INPUT:See in the figure 2.20.

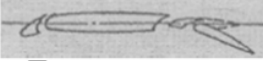
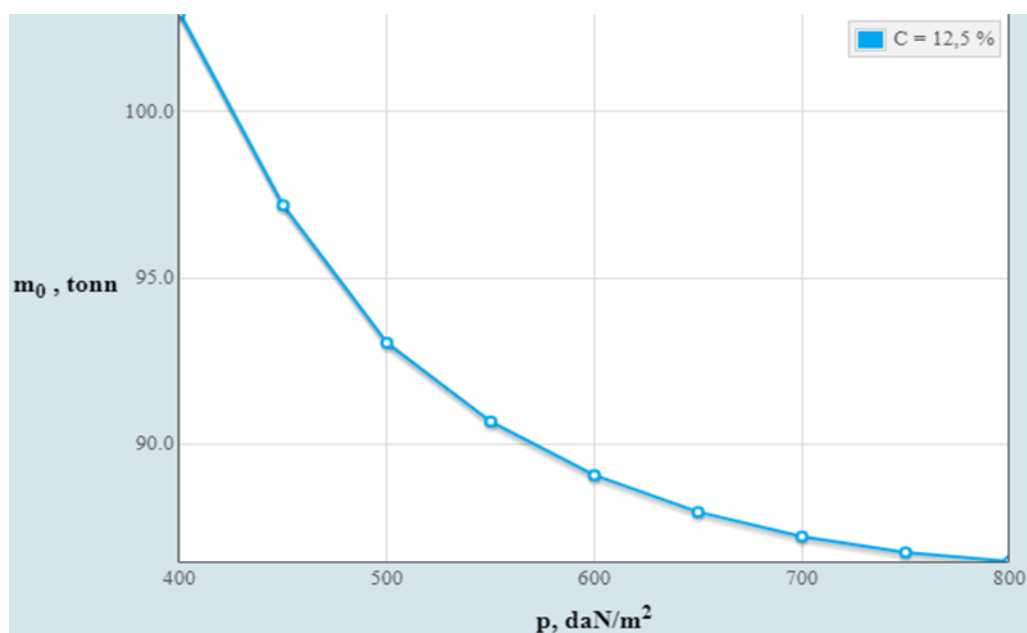
Airplane category selecting and it's parameters editing:		Airplane take-off mass	
Select airplane type: Passenger <input type="button" value="v"/>			
$n_{\text{pass. (itm.)}}$:	<input type="text" value="200"/>		
$m_{\text{pass. (kg)}}$:	<input type="text" value="100"/>		
Wing high-lift devices parameters:			
Choose wing high-lift devices type:		Slat and double sloted retractable flap <input type="button" value="v"/>	
			
$\Delta \bar{C}_{y1.dev.}$:	<input type="text" value="2"/>	$dC_y=1.800..2.200$	
$\bar{l}_{sl.}$:	<input type="text" value="0.7"/>		
$k_{sl.}$:	<input type="text" value="0.15"/>		
$\bar{b}_{fl.}$:	<input type="text" value="0.24"/>		
$\bar{b}_{fl.tab.}$:	<input type="text" value="0.300"/>		
$\delta_{fl.TO} \text{ (deg.)}$:	<input type="text" value="25"/>		
$\delta_{fl.TO.tabl.} \text{ (deg.)}$:	<input type="text" value="40.00"/>		
$\bar{l}_{fl.}$:	<input type="text" value="0.7"/>		
$k_{fl.}$:	<input type="text" value="0.15"/>		
Initial data:			
\bar{C} (%):	<input type="text" value="12.5"/>	λ_w :	<input type="text" value="9.45"/>
η :	<input type="text" value="6.3"/>	$\chi_{le} \text{ (deg.)}$:	<input type="text" value="25"/>
$\alpha_{TO} \text{ (deg.)}$:	<input type="text" value="9"/>	M_{TO} :	<input type="text" value="0.2"/>
$d_{fus.} \text{ (m)}$:	<input type="text" value="4"/>	$\lambda_{fus.}$:	<input type="text" value="10.2"/>
$k_{mid.} \text{ (daN/m}^2\text{)}$:	<input type="text" value="5000"/>	$k_{int.w.}$:	<input type="text" value="0.65"/>
$k_{stab.}$:	<input type="text" value="1.35"/>	$k_{pl.}$:	<input type="text" value="0.15"/>
\bar{h} :	<input type="text" value="0.75"/>	\bar{l} :	<input type="text" value="7"/>
$\bar{l}_{slots.}$:	<input type="text" value="0.75"/>	$n_{eng.} \text{ (itm.)}$:	<input type="text" value="2"/>
λ_n :	<input type="text" value="1.5"/>	$L_{TO} \text{ (m)}$:	<input type="text" value="2450"/>
$f_{tr.}$:	<input type="text" value="0.02"/>	$\tan(\Theta)$:	<input type="text" value="0.024"/>
$\gamma_{en.}$:	<input type="text" value="0.0203"/>	$L_c \text{ (km)}$:	<input type="text" value="5600"/>

Figure 2.20 - Initial data related to take-off mass

C_0 (%):	[?] 12.5	k_{fl} :	[?] 0.25
n_{cr} (itm.):	[?] 8	Choose wing panels type:	Conventional riveted panels
Choose fuel tanks type:		Choose fuel tanks type:	Soft fuel tanks in wing
Choose luggage accommodation type:		Choose luggage accommodation type:	Luggage in containers
Engine type selecting and dependant parameters editing:			
Choose engines configuration:		Choose engine type:	Under the wing and df<5m
y :	[?] 9		Turbo-fan/jet
$\xi_{int.}$:	[?] 0.98		
$\xi_{tr.cr.}$:	[?] 0.7		
$\xi_{tr.TO.}$:	[?] 0.98		
$M_{cr.}$:	[?] 0.84		
$H_{init.}$ (km):	[?] 12		
$H_{fin.}$ (km):	[?] 12		
k_1 :	[?] 0.25		
$n_{rev.eng}$ (itm.):	[?] 2		
$k_{f.e.}$:	[?] 0.023		
Stabilisers parameters:			
Choose stabiliser configuration:			Low positioned stabiliser
$S_{h.st.}$:	[?] 0.2367		
$S_{v.st.}$:	[?] 0.1244		
Landing gear parameters:			
Main landing gear attachment place (for turboprop):			All struts attached to the wing
Main landing gear struts attachment place:			Into the wing
Main landing gear wheels accommodation place:			In the fuselage
Main landing gear struts number:			Two main struts
Iterative computations parameters:			
Parameter being studied:			C - Airfoil relative thickness
Initial value:	[?] 8		
Final value:	[?] 14		
Increment:	[?] 0.5		
Initial p:	[?] 200		
Final p:	[?] 800		
Increment p:	[?] 50		

Figure 2.20 - Initial data related to take-off mass

RESULT: See in the figure 2.21.

Figure 2.21(a) - Diagram of m_0 and p

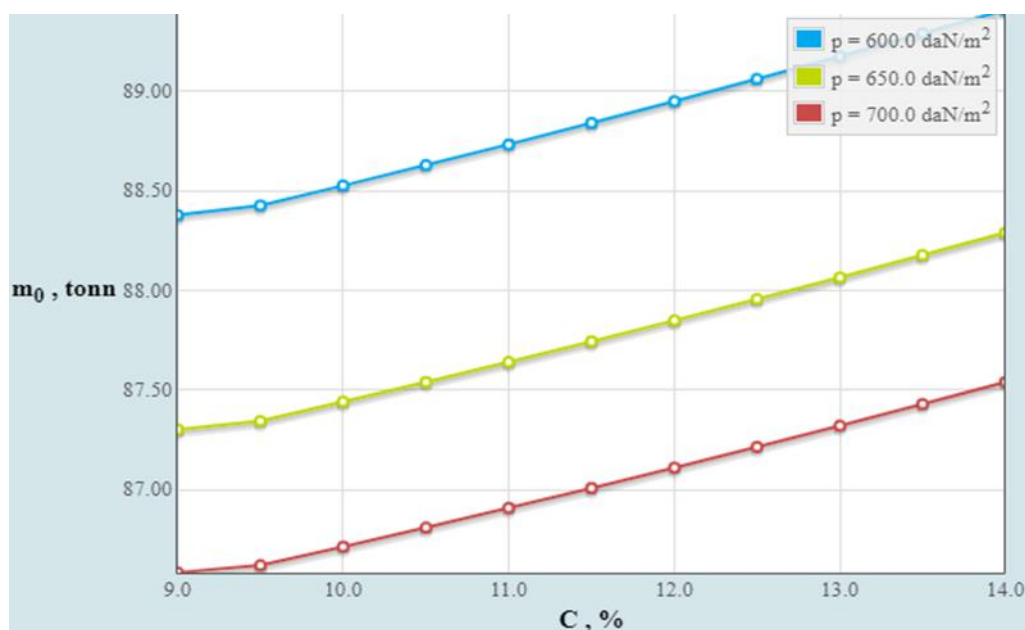


Figure 2.21(b) - Diagram of m_0 and C

CONCLUSION: This lab gives us the total take off mass of the aircraft. The take off mass of the aircraft obtained for wing loading 700 daN/m² and relative thickness of chord 12.5 is 87.2 Tons, the take off mass of the aircraft obtained is very high. Although the higher the value, the better, but if it is too high, it will cause damage to the force transmission structure of the aircraft and also affect the life of other components. Therefore, a reasonable upper limit value needs to be determined in future calculations.

3. ECONOMIC SECTION

3.1. Calculation of aircraft and engine operation cost and transportation cost of one cargo ton per kilometer.

The operating costs of this type of aircraft per 1:00 flight (flight hour) consist of direct and indirect (airport) expenses (formula (3.1)):

$$C_{OP} = A + B, \quad (3.1)$$

Where A - direct costs per flight hour, dollars;

B - Indirect costs per flight hour, dollars.

Direct costs include expenses for depreciation and overhaul and maintenance of an airplane (glider) and engines for fuel and flight personnel wages with accruals.

Indirect costs include depreciation, maintenance and maintenance of all aerodrome and airport facilities (bus stations, hotels, taxiways, parking lots, weather services, hangars, warehouses, roads, utilities, garages, etc.), excluding expenses for repair factories and linear workshops, as well as salary expenses for the payroll of GA units.

The total cost of operating the aircraft for the transport of passengers or commercial cargo per kilometer (CTKM) is determined by (formula (3.2)):

$$C_{TKM} = \frac{A+B}{m_{ld} \cdot k \cdot V_c} \quad (3.2)$$

Where m_{ld} = 20000 kg, is the maximum payload of the aircraft;

$V_c = 800 \text{ km / h}$ - airspeed;

$K = 0.65$ - utilization factor of the aircraft load.

The size of the speed of the aircraft is determined based on its cruising speed. Flight (technical) speed is the average speed of a non-stop flight in calm, calculated taking into account the time spent at all stages of the flight from the start of acceleration at the landing airport. Calculated speed by (formula (3.3)):

$$V_c = \frac{L \times V_{cr}}{L + (V_{cr} \times \Delta t)} \quad (3.3)$$

Where $V_{CR} = 830 \text{ km/hr}$ - cruising speed of the aircraft;

$L = 5600 \text{ km}$ - non-stop flight range;

$t = 0.25$ - loss of time for evolution or maneuvering in the airport area after take-off and before landing, as well as climb and decrease, which corresponds to a speed equal to cruising (in hours).

The magnitude of these losses depends on the altitude of the aircraft.

$$V_c = \frac{5600 \times 830}{5600 + (830 \times 0.25)} = 800 \text{ km/hr}$$

Direct expenses per one hour of flight; consist of the following expenses (formula (3.4)):

$$A = \sum_{i=1}^7 A_i \quad (3.4)$$

Where A_1 is the cost of depreciation and overhaul of the aircraft (glider)

A_2 - expenses for depreciation and overhaul of engines;

A_3 - maintenance and current repair costs for the airframe;

A4 - maintenance and current repair costs of power plants;

A5 - salary of flight personnel with accruals;

A6 - fuel cost;

A7 - other direct costs.

All A_i , we take per one flight hour.

The cost of depreciation and overhaul for one hour of aircraft operation, we define by (formula (3.5)):

$$A_1 = K_1 \times P_C \times \frac{1 + K_{RA} \times \left(\frac{T_C}{t_C} - 1 \right)}{T_C} \quad (3.5)$$

Where $K_1 = 1,065$ - coefficient taking into account non-productive raid (instruction, training, flight test, etc.).

P_C - price of an airplane without engines, dollars (formula (3.6)).

$$P_C = 0,015 \cdot K_{HBO} \cdot K_{CEP} \cdot K_V \cdot m_{ep} \cdot (3340 + 0,077 \cdot m_{ep} - 1,05 \cdot 10^{-5} \cdot m_{ep}^{1,5}) \quad (3.6)$$

Where, $K_{HBO} = 1,61$

$m_{eq} = m_{af} - (m_{CR} + m_{pp})$ - Mass of an empty plane.

$m_{af} = 49152$ kg - mass of the airframe;

$m_{CR} = 480$ kg — weight of the service load of the aircraft taking into account the weight of the crew;

$m_{pp} = 10240$ kg - mass of power plants;

$m_{eq} = 49152 - (480 + 10240) = 38432$ kg

Coefficient taking into account the seriality of the designed aircraft (formula (3.7));

$$K_{CEP} = \left(\frac{35 \cdot 10^5}{m_{ep} \cdot \sum n_C} \right)^{0,4} \quad (3.7)$$

Where $\sum n_C = 100$ – number of aircraft in a series;

$$K_{CEP} = \left(\frac{35 \cdot 10^5}{38432 \cdot 100} \right)^{0,4} = 0.963$$

Coefficient taking into account the estimated flight speed of the designed aircraft (formula (3.8)).

$$K_V = \frac{1}{2} \cdot \left(1 + \frac{v_{cr}}{800} \right) \quad (3.8)$$

Where $V_{cr} = 830$ km/h – aircraft cruising speed.

$$K_V = \frac{1}{2} \cdot \left(1 + \frac{830}{800} \right) = 1.019$$

$P_C = 0,015 * 1.61 * 0.963 * 1.019 * 38432 * (3340 + 0.077 * 38432 - 1.05 * 10^{-5} * 38432^{1.5}) = 5665154.55$ Dollars.

K_{RA} - coefficient showing the ratio of the cost of major repairs of the aircraft to the price of the aircraft (formula (3.9)).

$$\begin{aligned} K_{RA} &= 0,11 + (3 \cdot 10^4 / P_C) \quad (3.9) \\ &= 0,11 + 30000 / 5665154.55 \\ &= 0.1153 \end{aligned}$$

For main aircraft on average:

$$T_c = 30000 \text{ h};$$

$$t_c = 5000 \text{ h};$$

$$A_1 = 1.065 * 5665154.55 * \frac{1 + 0.1153 * \left(\frac{30000}{5000} - 1 \right)}{30000} = 317.05$$

Dollars/hour.

Depreciation and overhaul expenses at 1:00 of engine operation, dollars / h, are determined by (formula (3.10)):

$$A_2 = K_2 \cdot n_{en} \cdot P_{en} \cdot \frac{1 + K_{REN} \cdot \left(\frac{T_{en}}{t_{en}} - 1\right)}{T_{en}} \quad (3.10)$$

Where $K_2 = 1.07$ - coefficient taking into account non-production raid;

$n_{en} = 2$ - the number of engines installed on the plane;

P_{en} - price of one engine, dollars (formula (3.11)):

$$P_{EN} = 61,183 \cdot K_{HBO} \cdot N_{Emax} \quad (3.11)$$

Where $N_{Emax} = 26000$ kW - maximum engine power;

$$K_{HBO} = 1.61$$

$$P_{EN} = 61.183 \times 1.61 \times 26000 = 2561120.4 \text{ dollars.}$$

$$T_{en} = 6000 \text{ h;}$$

$$t_{en} = 3000 \text{ h;}$$

$$K_{REN} = 0.6;$$

$$A_2 = 1,07 * 2 * 2561120.4 * \frac{1 + 0.6 * \left(\frac{6000}{3000} - 1\right)}{6000} = 1461.6 \text{ Dollars /h.}$$

The costs of current repairs and maintenance of the airframe (A_3) and engines (A_4), dollars / h, consist of the costs of materials and spare parts, the wages of technical workers directly involved in the maintenance and repair of aircraft and engines, and are determined as follows (formula (3.12)):

$$A_3 = 0,024 \cdot K_3 \cdot K_4 \cdot (0,39 - 0,121 \cdot 10^{-5} \cdot m_{ep}) \cdot m_{ep} \quad (3.12)$$

Where $K_3 = 0.61$ - coefficient taking into account the maintenance

method;

$K_4 = 1$ - for aircraft with turbojet engine and turbofan engine;

$m_{eq} = 38432$ kg;

$A_3 = 0.024 * 0.61 * 1 * (0.39 - 0.121 * 10^{-5} * 38432) *$

$38432 = 193.27$ Dollars/h

$$A_4 = \frac{0,024 \cdot 16 \cdot K_2 \cdot K_5 \cdot n_{en} \cdot \sqrt{R_{max}}}{1 + 7 \cdot 10^{-5} \cdot T_{en}} \quad (3.13)$$

Where $K_2 = 1.07$ - coefficient taking into account non-production plaque;

$K_5 = 1$;

$R_{max} = N_{E_{max}} = 26000$ kW;

$T_{en} = 6000$ g.

$$A_4 = \frac{0,024 \cdot 16 \cdot 1.07 \cdot 1 \cdot 2 \cdot \sqrt{26000}}{1 + 7 \cdot 10^{-5} \cdot 6000} = 93.31 \text{ dollars / h}$$

The wage costs of flight personnel for one flight hour (A_5), dollars / h, we consider, based on the number of passenger seats (formula (3.14)):

$$A_5 = 1,5 \cdot (0,9 \cdot n_{pass} - 0,00237 \cdot n_{pass}^2 - 2,9 \cdot 10^{-6} \cdot n_{pass}^3) \quad (3.14)$$

Where $n_{pass} = 160$ people - the maximum possible number of passenger seats on this aircraft;

$$A_5 = 1.5 * (0.9 * 160 - 0,00237 * 160^2 - 2.9 * 10^{-6} * 160^3) = 107.2 \text{ Dollars / h}$$

The fuel costs attributable to 1:00 flight (A_6), dollars / h, we calculate by (formula (3.15)).

$$A_6 = 1,5 \cdot b \cdot P_k \cdot m_T \cdot n_{en} = \frac{m_T \cdot m_0}{t_{\Sigma} \cdot n_{en}} \times P_k \quad (3.15)$$

Where $m_T = 0.52$ - relative mass of fuel;

$m_0 = 204800$ kg - take-off mass of the aircraft;

$t_{\Sigma} = 6$ h - total flight time;

$P_k = \$ 1.5$ / kg - the price of kerosene;

$b = 1.045$ - coefficient taking into account productive fuel consumption.

$$A_6 = \frac{0.52 \cdot 204800}{6 \cdot 2} \times 1.5 = 13312 \text{ Dollars / h.}$$

Other expenses for the aircraft (formula (3.16)):

$$A_7 = 0,07 \cdot \sum_{i=1}^6 A_i \quad (3.16)$$

$$A_7 = 0.07 * (317.05 + 1461.6 + 193.27 + 93.31 + 107.2 + 13312) \\ = 1083.91 \text{ dollars / h.}$$

$$A_{\Sigma} = 317.05 + 1461.6 + 193.27 + 93.31 + 107.2 + 13312 + \\ 1083.91 = 16568.34 \text{ dollars / h.}$$

Indirect costs (B) include depreciation, maintenance and maintenance of all aerodrome and airport facilities and the salaries of ground personnel (except the salaries of technical workers engaged in the maintenance and repair of the aircraft fleet).

Indirect costs depend on the class of the airfield and the number of take-offs and landings per hour of flight.

Therefore, for this aircraft indirect costs will be (formula (3.17)).

$$B = 0.4 * A_{\Sigma} \quad (3.17)$$

$$= 0.4 \times 16568.34 = 6627.34 \text{ dollars / h.}$$

The operating costs of this aircraft per 1:00 flight (flight hour) are (formula (3.18)).

$$C_{OP} = A + B, \quad (3.18)$$

$$C_{OP} = 16568.34 + 6627.34 = 23195.68 \text{ dollars / h.}$$

The total cost of operating the aircraft for the transport of passengers and commercial cargo per kilometer is calculated by (formula (3.19)):

$$C_{TKM} = \frac{A+B}{m_{ld} \cdot k \cdot V_c} = \frac{23195.68}{20 \times 0.65 \times 800} = 64.33 \times 10^{-2} \text{ Dollars / TKm} \quad (3.19)$$

The revenue received by the aviation company from operating a fleet of aircraft of this type falls on one ton-kilometer, determined by (formula (3.20)):

$$R = \frac{P_B \times n_{pass} \times K_3}{m_{ld} \times V_c \times \tau} = \frac{850 \times 160 \times 0.61}{20 \times 800 \times 6} = 86.42 \times 10^{-2} \text{ Dollars / h.} \quad (3.20)$$

The profit earned by an aviation company from operating a fleet of aircraft of this type falls on one ton-kilometer, calculated by (formula (3.21)).

$$P_{rf} = R - C_{TKM} \quad (3.21)$$

$$P_{rf} = 86.42 \times 10^{-2} - 64.33 \times 10^{-2} = 22.09 \times 10^{-2} \text{ Dollars / TKm}$$

To determine the price of a ticket provided that the operation of an aircraft of this class is break-even. We write the formula in the form (formula (3.22)).

$$R = C_{TKM} + P_{rf}, \quad (3.22)$$

Where $P_{rf} = 0$ (break-even condition), Putting the unknown price of the ticket (CB) in revenue, we get:

$$P_B = \frac{m_{ld} \cdot V_C \cdot \tau \cdot C_{TKM}}{n_{pas} \cdot K_3} \quad (3.23)$$

$$P_B = \frac{20 \cdot 800 \cdot 6 \cdot 64.33 \cdot 10^{-2}}{160 \cdot 0.61} = 632.75 \text{ Dollars}$$

$$P_B = 632.75 \text{ Dollars}$$

With a margin of 25%, ticket price:

$$P_B = 1.25 \times 632.75 = 790.94 \approx 791 \text{ Dollars.}$$

3.2. Conclusion

In this economic section, I calculated the Costs of operation of my newly designed aircraft and its engines at 23195.68 dollars/h and the cost of the transportation of one ton of cargo per kilometer. I also determined the ticket price, which is equivalent to \$791. And lastly, the indirect costs for one hour of flight, which equated to 6627.34 dollars / h.

CONCLUSIONS

As a result of the implementation of the master's degree project by various research methods, the following results were obtained:

The main parameters and characteristics of analog aircraft are analyzed.

The takeoff mass of the projected aircraft was determined and amounted to 204800 kg. The masses of the main components of the aircraft, depending on the takeoff mass of the aircraft, were calculated; wing mass – 19464.2 kg; fuselage mass – 17252.4 kg; tailunit mass – 3391.5 kg; power plant mass – 10240 kg; landing gear mass – 9044kg; fuel mass – 106496 kg and payload – 20000 kg.

The basic geometric parameters of the projected jet trainer aircraft have been determined: $S= 111.72 \text{ m}^2$, $L_{\text{wing}}= 32.492 \text{ m}$, $L_{\text{fus}}= 40\text{m}$, $\eta= 6.3$, $\lambda =9.45$, $bA=4.04 \text{ m}$. the flight characteristics: $L=5600 \text{ km}$, $V_{\text{cruis}}=830 \text{ km/h}$.

Intelligent flexible adaptive wing structures are designed and kinematic principles are verified.

The direct and indirect costs were also calculated, and the transportation cost of one cargo ton per kilometer was calculated. Finally, the price of the ticket was arrived at and equated to 791 dollars.

REFERENCES

1. Advanced technology and development of high lift system for civil aircraft,[Electronic resource] , MA G J, AN G, SHI Y M,etAl, <http://hkxb.buaa.edu.cn>.
2. Development of a pilot project of an aircraft [text]: Training guide / A.K. Myalitsa, L.A. Malashenko, A.G. Grebenikov, E.T. Vasilevskiy, V.N. Klimenko, A.A. Serdyukov – Kharkiv: National Aerospace University Kharkov Aviation Institute, 2011. – 233 p.
3. Research and progress of green aviation technology [M]. SUN X S. Beijing: Aviation Industry Press, 2020 : 726-740.
4. Some Design Details of A350XWB[J]. International Aviation, MA Y. 2007, 08:15-17(in Chinese)
5. Review of High-lift Device Technology Development on Large Aircrafts[J]. Aeronautical Science & Technology, LI L Y. 2015, 5: 1-10(in Chinese).
6. The Aerodynamic Design of the A350XWB-900 High Lift System[C]. 29th International Congress of the Aeronautical Sciences, St. Petersburg, Russia, STRUBER H. 2014.
7. Research on the Status and Key Technology in Morphing Airfoil of Adaptive Wings[J]. Advances in Aeronautical Science and Engineering, NI Y G, YANG Y. 2018, 9(3): 297-308(in Chinese).

8. Design and application of compliant mechanisms for morphing aircraft structure[J]. Smart Structures and Materials 2003: Industrial and Commercial Applications of Smart Structures Technologies Proceedings of SPIE, Kota S, Hetrick J, Osborn R, et al. 2003, 5054, 24-33.
9. Realization of optimized wing camber by using formvariable flap structures[J]. Aerospace Science Technology, Monner H P. 2001, 5: 445-455.
10. Study on mechanical properties of new Zero Poisson ratio honeycomb structure and variable wing[D]. Harbin: Harbin Institute of Technology, HUANG J. 2018: II(in Chinese).
11. Future of aircraft wings: movable leading edge with flexible skin and integrated functions[N]. Press Release, Anke Zeidler- Finsel. 2015-6-1
12. Manufacturing and wind tunnel validation of a morphing compliant wing[J]. Journal of Aircraft, Alessandro D G, Luca P, Sergio R. 2018, 55(6): 231-2326.
13. Aero-servo-elastic design of a morphing wing trailing edge system for enhanced cruise performance [J]. Aerospace Science and Technology, Arena M, Antonio C, Rosario P. 2019, 86: 215-235.

14. Development status of key technologies and expectation about smart morphing aircraft[J]. Acta Aerodynamica Sinica, BAI P, CHEN Q, XU G Q, et al. 2019, 37(3): 426- 443(in Chinese).
15. Research on the Development and Key Technology of Smart Morphing Aircraft[J]. Tactical Missile Technology, XU Y T. 2017, (2): 26-33(in Chinese).
16. Realization of an optimized wing camber by using form variable flap structures[J].Aerospace Science Technology, Monner HP.2001,5:445~455
17. Study of controlled kinematics of the flexible rib of adaptive wing, xiejiang,yangzhichun